© 2018. Published by The Company of Biologists Ltd | Development (2018) 145, dev167379. doi:10.1242/dev.167379

RESEARCH ARTICLE

Distinct temporal requirements for Sonic hedgehog signaling in development of the tuberal hypothalamus

Tanya S. Corman, Solsire E. Bergendahl and Douglas J. Epstein*

ABSTRACT

Sonic hedgehog (Shh) plays well characterized roles in brain and spinal cord development, but its functions in the hypothalamus have been more difficult to elucidate owing to the complex neuroanatomy of this brain area. Here, we use fate mapping and conditional deletion models in mice to define requirements for dynamic Shh activity at distinct developmental stages in the tuberal hypothalamus, a brain region with important homeostatic functions. At early time points, Shh signaling regulates dorsoventral patterning, neurogenesis and the size of the ventral midline. Fate-mapping experiments demonstrate that Shh-expressing and -responsive progenitors contribute to distinct neuronal subtypes, accounting for some of the cellular heterogeneity in tuberal hypothalamic nuclei. Conditional deletion of the hedgehog transducer smoothened (Smo), after dorsoventral patterning has been established, reveals that Shh signaling is necessary to maintain proliferation and progenitor identity during peak periods of hypothalamic neurogenesis. We also find that mosaic disruption of *Smo* causes a non-cell autonomous gain in Shh signaling activity in neighboring wild-type cells, suggesting a mechanism for the pathogenesis of hypothalamic hamartomas, benign tumors that form during hypothalamic development.

KEY WORDS: Shh, Tuberal hypothalamus, VMH, DMH, Ventral midline, Cellular heterogeneity

INTRODUCTION

The hypothalamus is an ancient brain region with important roles in the regulation of several homeostatic processes and animal behaviors. Neural circuits mapping to distinct areas of the hypothalamus control a variety of essential bodily functions, including food intake, energy expenditure, fluid balance, temperature regulation, wakefulness, daily rhythms, as well as social behaviors associated with reproduction, aggression, arousal and stress (Saper and Lowell, 2014; Zha and Xu, 2015; Hashikawa et al., 2017; Tan and Knight, 2018). Organized into small clusters of neurons, termed nuclei, the hypothalamus is unlike other regions of the central nervous system (CNS) that are typically arranged in cell layers (Shimada and Nakamura, 1973; Altman and Bayer, 1986). Further adding to this complex architecture, most hypothalamic nuclei are composed of diverse neuronal cell types with opposing or sometimes unrelated functions. The developmental mechanisms regulating neuronal heterogeneity within hypothalamic nuclei are poorly understood compared with other CNS regions (Bedont et al., 2015; Burbridge et al., 2016; Xie and Dorsky, 2017).

The hypothalamus derives from the ventral diencephalon and can be divided into four principal regions from rostral to caudal: preoptic, anterior, tuberal and mammillary. Within the tuberal hypothalamus, neurons in the arcuate nucleus (ARC), ventromedial hypothalamic nucleus (VMH), dorsomedial hypothalamic nucleus (DMH) and paraventricular nucleus (PVN) integrate sensory information from the environment to elicit autonomic, endocrine and behavioral responses that maintain vital set points in the animal or adapt to various stressors (Saper and Lowell, 2014). In addition to receiving inputs from other brain regions, the positioning of the tuberal hypothalamus offers unique exposure to peripheral cues carried through the bloodstream that are presented to neurons at the median eminence.

Recent advances have been made in our understanding of the neuronal circuitry and function of tuberal hypothalamic nuclei. This is particularly true for the VMH, an elliptical nucleus located above the ARC and below the DMH (Fig. 1L). The VMH is subdivided into ventrolateral (VMH_{VL}), central (VMH_{C}) and dorsomedial (VMH_{DM}) regions, each with distinguishable gene expression profiles (Segal et al., 2005; McClellan et al., 2006; Kurrasch et al., 2007). Genetic, pharmacogenetic and optogenetic approaches have further delineated VMH neurons into functionally distinct categories. ERα-expressing neurons in the VMH_{VL} regulate sexually dimorphic features related to energy expenditure, reproductive behavior and aggression (Lin et al., 2011; Lee et al., 2014; Correa et al., 2015). By contrast, insulin receptor (IR)-expressing neurons in the VMH_{C} and leptin receptor (LEPR) neurons in the VMH_{DM} affect body weight regulation in both males and females (Dhillon et al., 2006; Klöckener et al., 2011). Steroidogenic factor 1 (SF1, officially designated Nr5a1)-positive neurons in the VMH_{DM} also influence behavioral responses to fear and anxiety (Silva et al., 2013; Kunwar et al., 2015).

Despite the progress in assigning functions to VMH neurons, we still know relatively little about how this nucleus forms and the process by which its subdivisions are established. During hypothalamic development, Nr5a1 is selectively expressed by all VMH neurons soon after they exit the cell cycle and undergo neurogenesis (Tran et al., 2003). Nr5a1 is required for the terminal differentiation of VMH neurons, as well as their coalescence into a nucleus with a distinct cytoarchitecture (Ikeda et al., 1995; Davis et al., 2004; Büdefeld et al., 2011). Consequently, mice lacking Nr5a1 in the VMH are obese, anxious and infertile (Majdic et al., 2002; Zhao et al., 2008; Kim et al., 2010). Additional cell type-specific factors acting upstream of Nr5a1 remain to be identified.

One signaling molecule that may help bridge the gap in knowledge concerning the ontogeny of VMH neurons is Sonic Hedgehog (Shh). Shh has been studied in several spatial and temporal contexts related to hypothalamic development. Shh signaling from the prechordal plate, which underlies the ventral forebrain at early stages of its development, is required for the

Department of Genetics, Perelman School of Medicine, University of Pennsylvania, Philadelphia, PA 19104-6145, USA.

*Author for correspondence (epsteind@pennmedicine.upenn.edu)

S.E.B., 0000-0002-2449-8822; D.J.E., 0000-0002-4274-4521

Received 7 May 2018; Accepted 20 September 2018

Development (2018) 145, dev167379. doi:10.1242/dev.167379

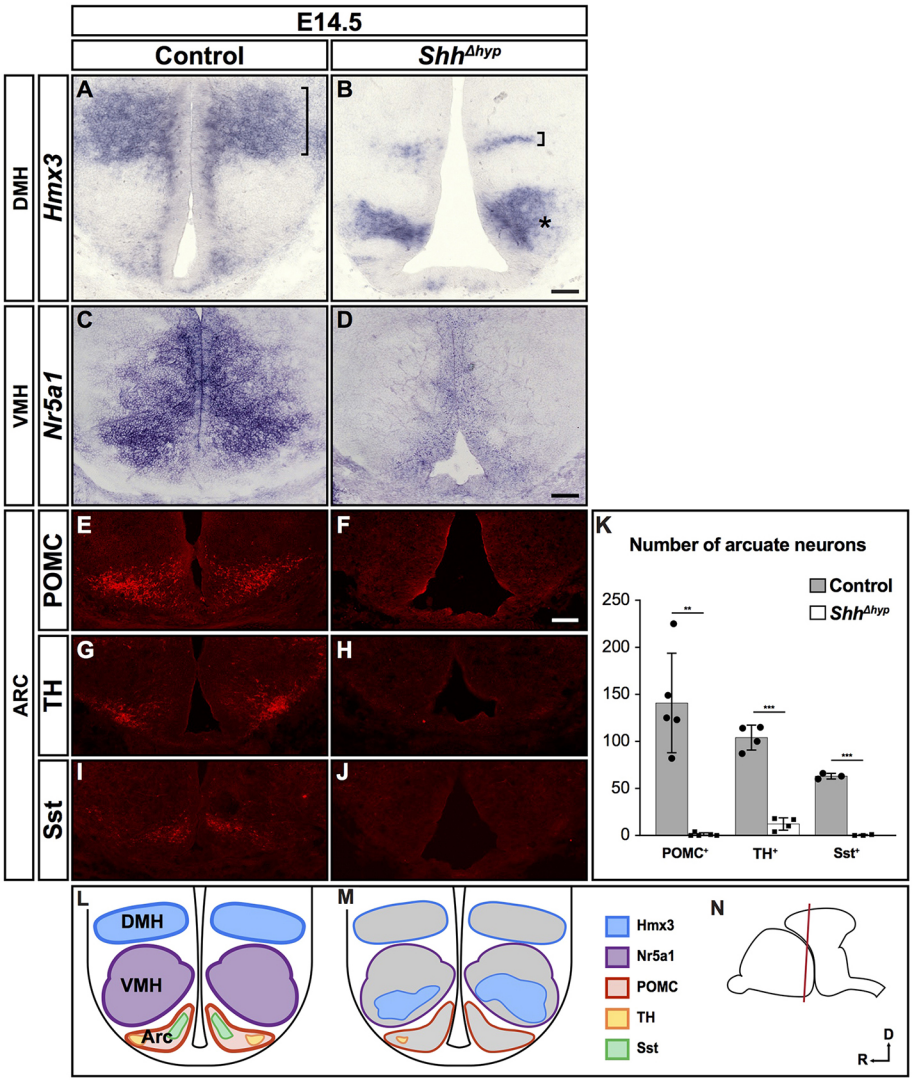

Fig. 1. Loss of tuberal hypothalamic neurons in *Shh*$^{\Delta hyp}$ embryos. Coronal sections through a caudal domain of the tuberal hypothalamus of control and *Shh*$^{\Delta hyp}$ embryos stained by RNA *in situ* hybridization (A-D) or immunofluorescence (E-J) at E14.5 for neuronal markers. (A,B) *Hmx3* is expressed in the DMH of control embryos, and shows reduced (bracket) and ectopic (asterisk) expression in *Shh*$^{\Delta hyp}$ mutants (n=3). (C,D) *Nr5a1* marks the VMH in control embryos and is absent in *Shh*$^{\Delta hyp}$ mutants (n=4). (E-K) The numbers of cells expressing markers of distinct neuronal subtypes in the ARC (POMC, TH and Sst) are reduced in *Shh*$^{\Delta hyp}$ mutants (n=5 for POMC, **P=0.0004; n=4 for TH, ***P<0.0001; n=3 for Sst, ***P<0.0001). Error bars indicate s.d. Each data point represents the number of cells expressing a given marker on a single section at equivalent levels of the tuberal hypothalamus (see Materials and Methods) from a single embryo (n=number of embryos analyzed). Statistical analysis was performed using a two-tailed unpaired t-test. (L,M) Schematics of coronal sections through the tuberal hypothalamus of control and *Shh*$^{\Delta hyp}$ embryos showing nuclei and cell type-specific markers. (N) Sagittal diagram of the brain showing plane of section (red line) in L,M. Scale bars: 100 µm.

induction of the hypothalamic territory (Chiang et al., 1996; Dale et al., 1997). Conditional deletion of Shh in the ventral diencephalon causes defects in the patterning, regionalization and formation of ventral hypothalamic nuclei (Szabó et al., 2009; Shimogori et al., 2010; Zhao et al., 2012; Carreno et al., 2017). Nevertheless, the pathogenic mechanisms underlying these Shh dependent alterations in hypothalamic development have yet to be fully elucidated. Moreover, since Shh continues to be expressed in VMH progenitors well beyond the initial patterning stage, additional roles for Shh in VMH nucleogenesis and neuronal subtype identity are likely (Alvarez-Bolado et al., 2012).

Here, we use conditional knockout mice to interrogate the functional requirements for Shh signaling at specific periods of hypothalamic development. We show that the pronounced loss of hypothalamic nuclei that manifests from early deletion of Shh at embryonic day 9 (E9.0) is caused by defects in dorsoventral patterning, neurogenesis and the expansion of ventral midline cells, indicating a novel role for Shh in restricting ventral midline development in the tuberal hypothalamus. Fate-mapping experiments reveal that Shh-expressing and Shh-responsive cell lineages are enriched in distinct domains of the VMH, contributing to the neuronal heterogeneity of this nucleus. Deletion of smoothened (Smo), an essential transducer of Shh signaling, at later stages of hypothalamic development (after E10.5), resulted in a cell-autonomous loss of VMH neuronal subtype identity. Remarkably, we also detect a non-cell-autonomous expansion and reprogramming of neighboring wild-type cells, which likely occurred in response to residual Shh ligand that was not taken up by *Smo* mutant cells. This gain in Shh signaling activity may explain the pathogenesis of hypothalamic hamartomas (HH), benign tumors caused, in some cases, by somatic gene mutations that block Shh responsiveness (Saitsu et al., 2016; Hildebrand et al., 2016).

RESULTS

Shh is required for development of tuberal hypothalamic nuclei

To determine how Shh signaling contributes to the formation of tuberal hypothalamic nuclei, we first evaluated the expression of cell type-specific markers in *SBE2-cre; Shh*$^{loxp/-}$ (*Shh*$^{\Delta hyp}$) embryos. *SBE2-cre* is a transgenic mouse line that uses Shh brain enhancer 2 (SBE2) to activate *cre* transcription in the ventral diencephalon in a similar pattern to the endogenous expression of *Shh*. We have previously shown that Shh is selectively deleted in the ventral diencephalon of *Shh*$^{\Delta hyp}$ embryos by E9.0 (Zhao et al., 2012). Expression of cell type-specific markers of the DMH (Hmx3), VMH (Nr5a1) and ARC (pro-opiomelanocortin, POMC; tyrosine hydoxylase, TH; and somatostatin, Sst) nuclei was either absent or greatly diminished in *Shh*$^{\Delta hyp}$ embryos at E14.5

Development (2018) 145, dev167379. doi:10.1242/dev.167379

(Fig. 1A-K; POMC-expressing cells: control 140.8±52.9, $Shh^{\Delta hyp}$ 1.0±1.7, n=5, P=0.0004; TH-expressing cells: control 104.0±13.2, $Shh^{\Delta hyp}$ 12.3±6.6, n=4, P<0.0001; Sst-expressing cells: control 63.0±3.0, $Shh^{\Delta hyp}$ 0.3±0.6, n=3, P<0.0001). Ectopic expression of *Hmx3* was also detected in the VMH, possibly owing to its derepression in the absence of Shh (Fig. 1A,B). These results are consistent with previous findings demonstrating a requirement for Shh in the development of tuberal hypothalamic nuclei (Fig. 1L-N; Szabó et al., 2009; Shimogori et al., 2010; Carreno et al., 2017).

Alterations in dorsoventral patterning, neurogenesis and ventral midline formation explain the absence of tuberal hypothalamic nuclei in $Shh^{\Delta hyp}$ embryos

Shh signaling is required to establish distinct neuronal identities at ventral positions along the length of the vertebrate neural tube through activation and repression of homeodomain and basic helix-loop-helix (bHLH) transcription factors (Ericson et al., 1997; Briscoe and Ericson, 1999; Briscoe et al., 2000; Muhr et al., 2001; Balaskas et al., 2012). However, the temporal and spatial dynamics of Shh signaling in the hypothalamus differ from those in more posterior regions of the CNS. *Shh* is initially broadly expressed in ventral hypothalamic progenitors and then rapidly downregulated in the ventral midline at the level of the tuberal hypothalamus (Manning et al., 2006; Trowe et al., 2013). As a result, *Shh* is expressed in bilateral stripes adjacent to the ventral midline, unlike in spinal cord and hindbrain regions where *Shh* is restricted to the floor plate (Fig. 2A; Echelard et al., 1993). Moreover, neural progenitors immediately dorsal to the bilateral stripes of *Shh* are responsive to Shh signaling, indicated by *Gli1* expression, whereas progenitors located in the ventral midline are refractory to Shh signaling (Fig. 2B; Ohyama et al., 2008).

We evaluated key patterning genes in $Shh^{\Delta hyp}$ mutants at E10.5 to address whether alterations in their expression might explain the loss of tuberal hypothalamic nuclei at later stages. As expected, *Shh* and *Gli1* were absent in $Shh^{\Delta hyp}$ embryos (Fig. 2A,B,H,I). The number of cells expressing Nkx2.1, a broad determinant of ventral hypothalamic progenitor identity (Kimura et al., 1996; Sussel et al., 1999), was reduced by 48% in $Shh^{\Delta hyp}$ embryos compared with control littermates (Fig. 2C,J,O; control: 540.8±56.4, n=5; $Shh^{\Delta hyp}$: 282.0±22.0, n=6, P<0.0001). In addition, Pax6, a prethalamic marker was expanded ventrally to a position abutting the Nkx2.1 domain (Fig. 2C,J). At E10.5, Nkx2.2 is expressed in a population of Shh-responsive neuronal progenitors that occupy the gap between cells expressing Pax6 and Nkx2.1 (Fig. 2D). The number of progenitor cells expressing Nkx2.2 in the ventricular zone of $Shh^{\Delta hyp}$ embryos was dramatically reduced (Fig. 2D,K,P; control: 221.0±21.2, n=4; $Shh^{\Delta hyp}$: 1.6±2.1, n=5, P<0.0001), which may explain the ventral expansion of Pax6 due to deficient cross-repressive interactions between these transcription factors (Ericson et al., 1997; Briscoe and Ericson, 1999; Muhr et al., 2001). These results suggest that alterations in the dorsoventral patterning of tuberal hypothalamic progenitors are responsible, at least in part, for the loss of their neuronal identities at later stages in $Shh^{\Delta hyp}$ embryos.

The bHLH transcription factor Ascl1 is required for ARC and VMH neurogenesis (McNay et al., 2006). We observed an 81% reduction in the number of Ascl1-expressing cells in the ventral hypothalamus of $Shh^{\Delta hyp}$ embryos compared with control littermates (Fig. 2E,L,Q; control: 252.7±11.7, n=3; $Shh^{\Delta hyp}$: 47.0±18.5, n=3, P<0.0001). Therefore, the reduction of neuroendocrine neurons in the ARC and VMH nuclei of $Shh^{\Delta hyp}$ embryos may also be explained by the downregulation of Ascl1.

Another striking feature of $Shh^{\Delta hyp}$ embryos is the dysmorphic appearance of the ventral midline. Rather than the V-shaped morphology typical of wild-type embryos, the ventral midline of $Shh^{\Delta hyp}$ embryos is U-shaped with a flattened appearance (Fig. 2F,M). Ventral midline cells in the tuberal hypothalamus

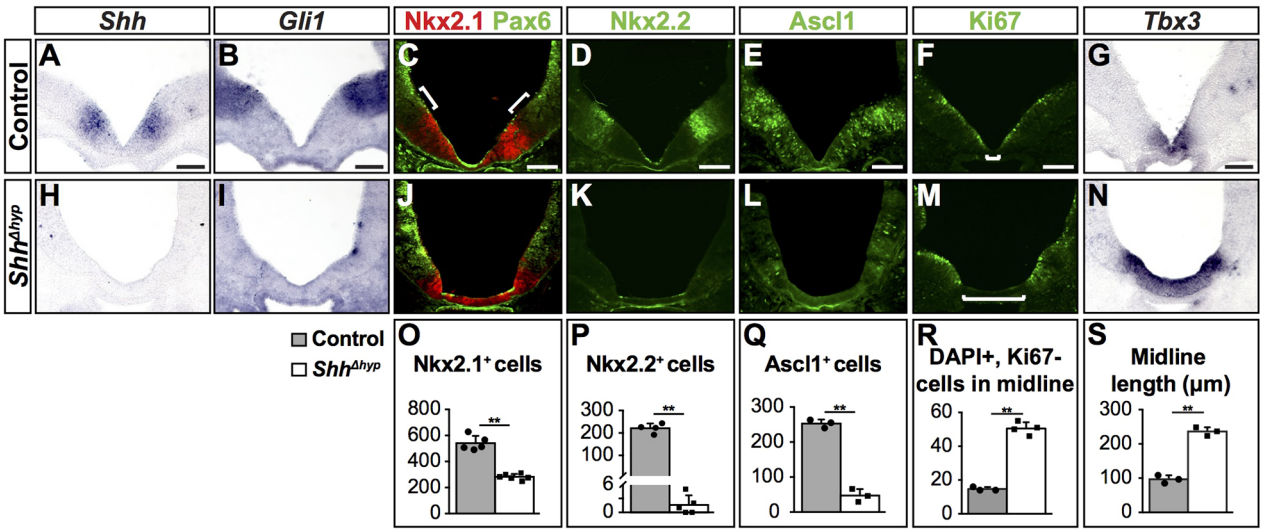

Fig. 2. Altered dorsoventral patterning, neurogenesis and ventral midline development in $Shh^{\Delta hyp}$ embryos. Coronal sections through control and $Shh^{\Delta hyp}$ embryos stained by RNA *in situ* hybridization (A,B,G-I,N) or immunofluorescence (C-F,J-M) at E10.5. (A,H) *Shh* expression in the prospective tuberal hypothalamus is lost in $Shh^{\Delta hyp}$ mutants (n=3). (B,I) *Gli1* expression in neuronal progenitors immediately dorsal to *Shh* is absent in $Shh^{\Delta hyp}$ mutants (n=3). (C,J,O) The number of cells in the ventral hypothalamus expressing Nkx2.1 is reduced in $Shh^{\Delta hyp}$ mutants (n=5 for controls, n=6 for $Shh^{\Delta hyp}$), whereas the domain of Pax6 expression is expanded ventrally. The gap between Nkx2.1 and Pax6 (white bracket) in control embryos is missing in $Shh^{\Delta hyp}$ mutants. (D,K,P) The number of Nkx2.2-expressing cells in tuberal hypothalamic progenitors is greatly reduced in $Shh^{\Delta hyp}$ mutants (n=4 for controls, n=5 for $Shh^{\Delta hyp}$). (E,L,Q) The number of Ascl1-expressing neurogenic progenitors is reduced in $Shh^{\Delta hyp}$ mutants (n=3). (F,M,R) The number of non-proliferating ventral midline cells identified by the absence of Ki67 staining (white brackets) is expanded in $Shh^{\Delta hyp}$ mutants (n=4). (G,N,S) The expression of *Tbx3* in the ventral midline is expanded in $Shh^{\Delta hyp}$ mutants (n=3). Scale bars: 100 µm. For all quantifications, error bars indicate s.d. Each data point represents the number of cells expressing a given marker per section from a single embryo (n=number of embryos analyzed). Statistical analysis was performed using a two-tailed unpaired *t*-test (**P<0.0001).

Development (2018) 145, dev167379. doi:10.1242/dev.167379

undergo cell-cycle arrest and express the T-box protein Tbx3 in response to Bmp signaling (Manning et al., 2006; Trowe et al., 2013). We quantified the zone of non-proliferation by counting the number of DAPI-positive nuclei in the Ki67-negative ventral midline territory and observed a significant increase in $Shh^{\Delta hyp}$ embryos (Fig. 2F,M,R; 50.5±3.7, n=4) compared with control littermates (14.67±1.5, n=3, P<0.0001). The length of the ventral midline territory marked by Tbx3 was also significantly increased in $Shh^{\Delta hyp}$ embryos (Fig. 2G,N,S; 239.1±8.2 µm, n=3) compared with control littermates (96.7±11.6 µm, n=3, P=0.0001). These results demonstrate that the loss of Shh in the tuberal hypothalamus expands the fate of non-dividing ventral midline cells at the expense of proliferating Nkx2.1-positive neuronal progenitors. Interestingly, *Bmp4* was previously shown to be upregulated in the ventral midline of $Shh^{\Delta hyp}$ embryos (Zhao et al., 2012). Hence, our findings highlight a unique role for Shh in restricting the size of the ventral midline in the tuberal hypothalamus by opposing Bmp signaling, in stark contrast to the floor plate promoting activity of Shh in more posterior regions of the CNS (Echelard et al., 1993; Roelink et al., 1994; Roelink et al., 1995; Martí et al., 1995; Ericson et al., 1996; Chiang et al., 1996).

Descendants of *Shh*-expressing progenitors contribute to the VMH

Shh and *Gli1* continue to be expressed beyond the stage when tuberal hypothalamic progenitors first acquire their identity and extend into the peak period of DMH, VMH and ARC neurogenesis between E12.5 and E14.5 (Fig. S1). We next sought to determine the relative contributions of Shh-expressing and Shh-responsive progenitors to distinct tuberal hypothalamic nuclei. We used a genetic fate-mapping strategy to indelibly label Shh-expressing (Shh^{CreER}) and Shh-responsive ($Gli1^{CreER}$) progenitors with an inducible GFP reporter ($Rosa^{ZsGreen}$). Pregnant dams carrying either $Shh^{CreER/+}$; $Rosa^{ZsGreen/+}$ or $Gli1^{CreER/+}$; $Rosa^{ZsGreen/+}$ embryos were administered tamoxifen at a single time point: E10.5. The contribution of *Shh*- and *Gli1*-expressing cells to tuberal hypothalamic nuclei was evaluated by co-labeling with GFP and cell type-specific markers at E14.5.

The majority of postmitotic neurons in the VMH express Nr5a1 and Nkx2.1 at E14.5 (Fig. 3A,B; Correa et al., 2015). GFP^+ cells in $Shh^{CreER/+}$; $Rosa^{ZsGreen/+}$ embryos were detected in the ventricular zone adjacent to the VMH as well as in 46% of Nr5a1-positive neurons in the mantle zone (Fig. 3A,G). This finding suggests that *Shh*-expressing progenitors in the ventricular zone of the tuberal hypothalamus migrate radially to populate neurons in the VMH, in agreement with a previous study (Alvarez-Bolado et al., 2012). The number of GFP and Nr5a1 double-labeled neurons was enriched in ventral (199.3±11.9, n=3) compared with dorsal (112.3±8.0, n=3, P=0.0005) regions of the VMH in $Shh^{CreER/+}$; $Rosa^{ZsGreen/+}$ embryos (Fig. 3A and Fig. S2). A similar ventral VMH bias was observed for GFP and Nkx2.1 double-labeled neurons (Fig. 3B). Nkx2.2 is expressed in a subset of postmitotic neurons in the dorsal VMH, of which 22% co-label with GFP (Fig. 3C,G). These data

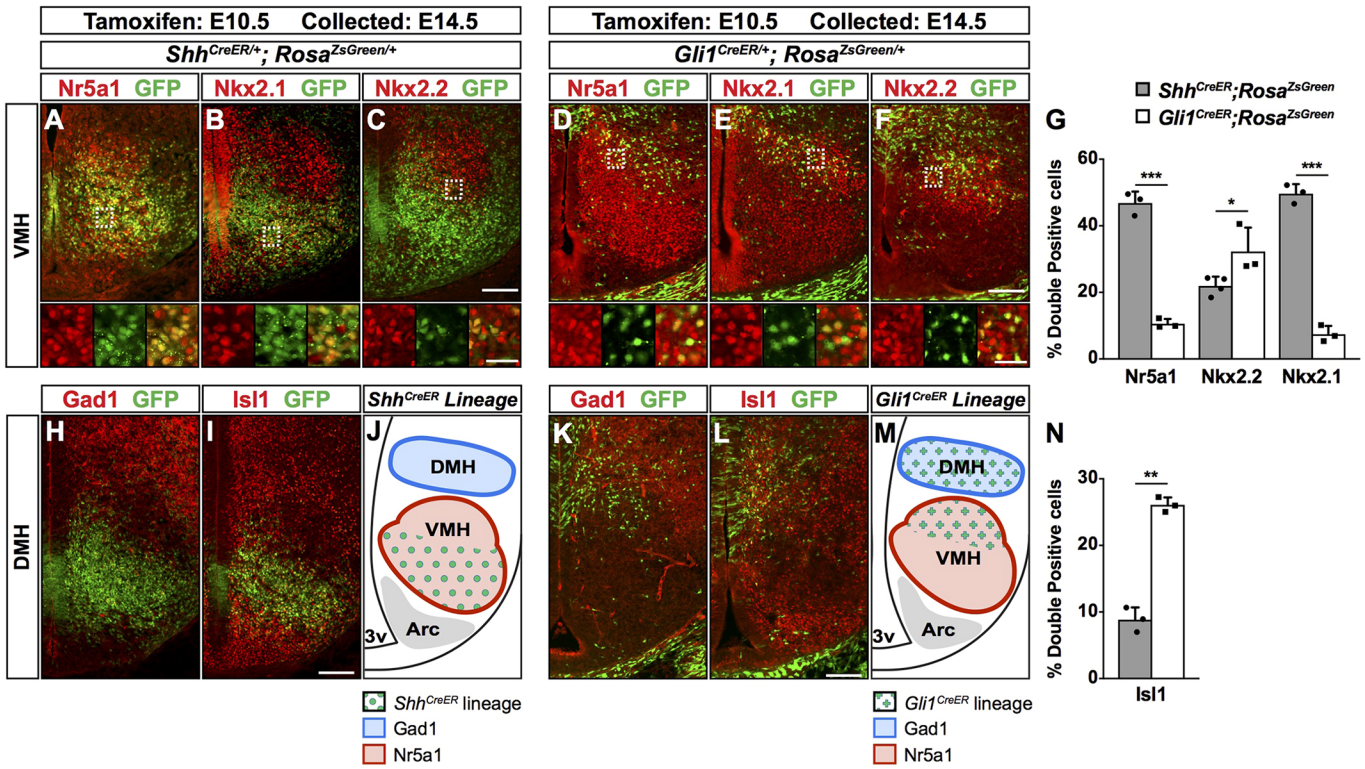

Fig. 3. *Shh*- and *Gli1*-expressing cells contribute to overlapping and distinct tuberal hypothalamic nuclei. Coronal sections through the tuberal hypothalamus of $Shh^{CreER/+}$; $Rosa^{ZsGreen/+}$ at the midpoint of the VMH. (A-C,H,I) and $Gli1^{CreER/+}$; $Rosa^{ZsGreen/+}$ (D-F,K,L) embryos at E14.5 that received tamoxifen at E10.5. The fate of *Shh*- and *Gli1*-expressing cells was determined by co-labeling with GFP (ZsGreen) and cell type-specific markers of the VMH and DMH. Insets in A-F are higher magnification views of boxed regions showing single- and double-labeled cells. (G,N) Quantification of fate-mapping experiments displayed as the proportion of double-positive cells (from either Shh or Gli1 lineages) to the total number of cells expressing a given marker: Nr5a1 (***P<0.0001, n=3); Nkx2.2 (*P=0.038, n=4 for Shh lineage, n=3 for Gli1 lineage); Nkx2.1 (***P<0.0001, n=3); and Isl1 (**P<0.0003, n=3). (J,M) Schematics demonstrating the contribution of *Shh*- and *Gli1*-expressing cell lineages to tuberal hypopthalamic nuclei. Scale bars: 100 µm; 25 µm in insets. Error bars indicate s.d. Each data point represents the number of cells expressing a given marker on a single hemi-section at equivalent levels of the tuberal hypothalamus (see Materials and Methods) from a single embryo (n=number of embryos analyzed). Statistical analysis was performed using a two-tailed unpaired t-test on arcsin-transformed data.

Development (2018) 145, dev167379. doi:10.1242/dev.167379

reveal that descendants of Shh-expressing progenitors marked with GFP at E10.5 are partitioned along the dorsoventral axis of the VMH into primarily ventral and central positions and are largely excluded from the dorsal-most region (Fig. 3J and Fig. S2).

We also assessed the contribution of Shh-expressing progenitors to other tuberal hypothalamic nuclei. The DMH is composed of GABAergic neurons that express Gad1 and a subset of neurons that express Isl1. No overlap in GFP and Gad1 or Isl1 was observed in the DMH of $Shh^{CreER/+}$; $Rosa^{ZsGreen/+}$ embryos, suggesting that Shh-expressing progenitors do not contribute to this nucleus when labeled at E10.5 (Fig. 3H-J). Some overlap between GFP and Isl1 was observed in ventrolateral neurons in the VMH, as well as a small subset of ARC neurons (Fig. 3I,N). In summary, Shh-expressing neuronal progenitors in the tuberal hypothalamus predominantly contribute to the VMH when labeled at E10.5.

Descendants of *Gli1*-expressing progenitors contribute to the DMH and VMH

We next examined the fate of Shh-responsive cells in $Gli1^{CreER/+}$; $Rosa^{ZsGreen/+}$ embryos administered tamoxifen at E10.5 and collected at E14.5. Given that *Gli1* is expressed dorsal to *Shh*, we expected that GFP^+ cells would be confined to the DMH. Indeed, GFP^+ cells were detected in the ventricular zone immediately adjacent to the DMH, as well as in Gad1- and Isl1-expressing neurons that appeared to migrate radially into the DMH (Fig. 3K-N).

Surprisingly, we also identified a small population of Nr5a1 neurons in the VMH of $Gli1^{CreER/+}$; $Rosa^{ZsGreen/+}$ embryos that co-labeled with GFP (Fig. 3D,G; 10.6±1.4%, n=3). These GFP^+ cells appeared to stream ventrally from a more-dorsal progenitor domain to occupy a dorsolateral region of the VMH (Fig. 3D-F). The number of GFP and Nr5a1 double-labeled neurons was enriched in dorsal (57.3±13.5, n=3) compared with ventral (5.0±1.7, n=3, P=0.002) regions of the VMH in $Gli1^{CreER/+}$; $Rosa^{ZsGreen/+}$ embryos (Fig. 3D and Fig. S2). GFP co-labeling was also observed in postmitotic neurons expressing Nkx2.1 and Nkx2.2 in primarily dorsal regions of the VMH (Fig. 3E-G). These data suggest that VMH neurons originate from spatially segregated pools of Shh-expressing and Shh-responsive progenitors that may contribute to the cellular heterogeneity of the VMH (Fig. 3J,M).

Shh signaling is required to maintain tuberal hypothalamic progenitors in a proliferative state

The results of our lineage-tracing and gene expression experiments demonstrated that Shh signaling is active in tuberal hypothalamic progenitors after their dorsoventral identity is established. To address whether Shh signaling is also required at later stages of DMH and VMH neurogenesis, we generated mice in which *Smo*, an essential regulator of Shh signaling, was conditionally deleted in *Gli1*-expressing cells at E10.5. This approach is expected to block Shh signaling in tuberal hypothalamic progenitors that are Shh responsive at E10.5.

Pregnant dams carrying $Gli1^{CreER/+}$; $Smo^{loxp/-}$; $Rosa^{ZsGreen/+}$ (*cSmo*) and $Gli1^{CreER/+}$; $Smo^{loxp/+}$; $Rosa^{ZsGreen/+}$ (control) embryos were administered tamoxifen at E10.5 and collected at different developmental stages. Strikingly, the number of GFP-positive cells in the tuberal hypothalamus was decreased by 43% in *cSmo* embryos (453.8±52.27, n=8) compared with control littermates (800.2±155.3, n=9, P=0.0003) when harvested at E14.5 (Fig. 4A-C). The reduction in GFP-positive cells was detected in both mantle and ventricular zones. A significant reduction in the number of GFP-positive cells was also observed 1 day earlier at E13.5 (Fig. 4D-F; *cSmo*: 418.1±45.5, n=7, versus control: 603±138.9, n=6, P=0.0066), but not at E12.5 (Fig. 4G-I; *cSmo*: 512.4±96.1, n=5, versus control: 578.6±96.7, n=5, P>0.05).

The failed expansion of Shh-responsive cells in *cSmo* embryos between E12.5 and E14.5 might be explained by increased cell death or decreased proliferation, or both. Immunostaining for activated caspase 3, an indicator of apoptosis, was minimal in *cSmo* and control embryos at E12.5 and E14.5, with no significant differences between genotypes (Fig. S3). On the other hand, fewer GFP-positive cells co-labeled with the proliferation marker Ki67 in the ventricular zone of *cSmo* embryos at E12.5 (Fig. 4J-L; 28.5±6.2%, n=3) compared with control littermates (50.1±8.7%, n=9, P=0.0249). From these results, we conclude that Shh signaling is required to maintain tuberal hypothalamic progenitors in a mitotically active state during the peak period of VMH and DMH neurogenesis.

Cell-autonomous requirement for Smo in promoting tuberal hypothalamic neuron identity

Given the contribution of Shh-responsive cells to distinct neuronal subtypes in the DMH and VMH, we next assessed whether aspects of their identity were compromised in *cSmo* mutants. We observed a 30% reduction in the number of Isl1-positive neurons in the DMH of *cSmo* (Fig. 5A-C; 477.6±130.7, n=5) compared with control littermates (678.3±44.6, n=4, P=0.0229). There was also a 30% reduction in the number of postmitotic neurons expressing Nkx2.2 in the dorsal VMH of *cSmo* (Fig. 5D-F; 315.2±52.1, n=9) compared with control embryos (451.6±28.2, n=9; P<0.0001). These findings suggest that the conditional loss of Shh signaling after E10.5 causes a cell-autonomous reduction in the proliferation of progenitors contributing to distinct DMH and VMH neurons.

Non-cell-autonomous defects in *cSmo* embryos alter VMH neuron subtype identity

Remarkably, despite the reduction of postmitotic neurons expressing Nkx2.2 in the VMH of *cSmo* embryos, the total number of VMH neurons expressing Nr5a1 was unchanged (Fig. 5G-I; *cSmo*: 598.5±100.7, n=8, versus control: 590.8±196.4, n=6, P=0.9253). Moreover, fewer Nr5a1-expressing neurons were found to co-label with Nkx2.1 in *cSmo* embryos, especially in ventral VMH regions (Fig. 5J-L, Fig. S4). The presence of defects in areas of the tuberal hypothalamus that are not derived from *Gli1*-expressing progenitors, such as VMH_{VL}, suggests that some phenotypes in *cSmo* embryos may occur through non-cell-autonomous mechanisms.

To address how non-cell-autonomous defects may be occurring in *cSmo* embryos, we evaluated the specification of tuberal hypothalamic progenitors. At E14.5, Nkx2.1 continues to be expressed in neuronal progenitors in the ventricular zone of the tuberal hypothalamus, extending from the ventral midline to a dorsal limit that approximates the border between the VMH and DMH (Fig. 6A). The ventral limit of Nkx2.2 expression in the ventricular zone overlaps with Nkx2.1 at the level of the dorsal VMH and extends caudally into the ventricular zone of the prethalamus (Fig. 6A).

We observed a significant reduction in the number of neuronal progenitors expressing Nkx2.1 in the ventricular zone of *cSmo* embryos (Fig. 6A; *cSmo*: 131.0±80.4, n=5, versus control: 259.4±58.9, n=5, P=0.0205) and a concomitant gain in the number of neuronal progenitors expressing Nkx2.2 (Fig. 6A; *cSmo*: 118.2±42.9, n=9, versus control: 58.0±23.2, n=9, P=0.002). The ventral expansion of Nkx2.2-positive progenitors was puzzling given our prior finding that postmitotic VMH neurons expressing

Development (2018) 145, dev167379. doi:10.1242/dev.167379

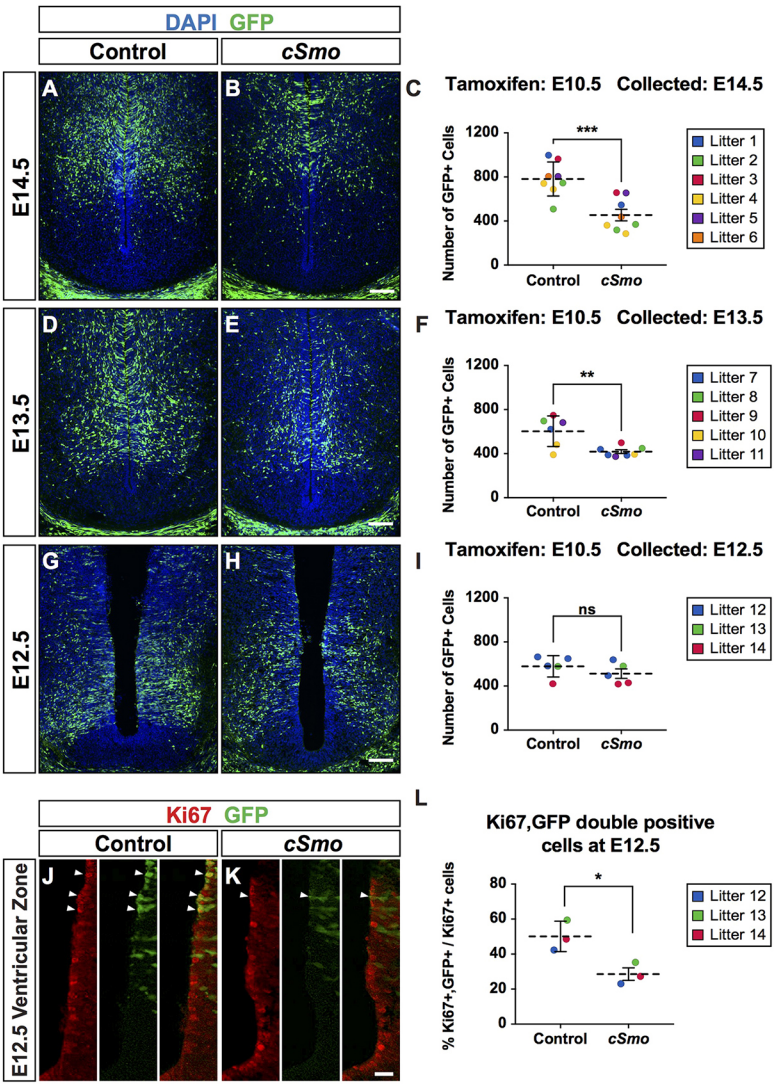

Fig. 4. Shh signaling is required for proliferation of tuberal hypothalamic progenitors. Coronal sections through the tuberal hypothalamus at the mid-point of the VMH of control and *cSmo* embryos at E14.5 (A,B), E13.5 (D,E) and E12.5 (G,H,J,K) that received tamoxifen at E10.5. (A-H) GFP (ZsGreen) fluorescence is shown on sections counterstained with DAPI. (C,F,I) Quantification of the number of GFP-positive cells from *cSmo* and control embryos tracked by litter. (J-L) Co-labeling of GFP and Ki67 (arrowheads) in the ventricular zone reveals a reduction in the number of proliferating GFP-positive cells in *cSmo* embryos at E12.5, as quantified in L. Scale bars: 100 µm in A-H; 25 µm in J,K. For all graphs, horizontal dotted line represents the mean and error bars indicate s.d. Each data point represents the number of cells expressing a given marker on a single hemi-section at equivalent levels of the tuberal hypothalamus from a single embryo color-coded by litter. Statistical analysis was performed using a two-tailed unpaired *t*-test (***P=0.0003, **P=0.0066, *P=0.0249).

Nkx2.2 were reduced in *cSmo* embryos (Fig. 5D-F). To reconcile these seemingly incongruous results, we reasoned that if a cell-autonomous loss of Shh signaling explains the reduction in Nkx2.2-positive neurons in the dorsal VMH, then perhaps a non-cell autonomous gain in Shh signaling could explain the increase in Nkx2.2-positive neuronal progenitors in more ventral regions of the tuberal hypothalamus.

Given that Nkx2.2 is a direct transcriptional target of Shh signaling (Lei et al., 2006; Vokes et al., 2007), we focused our attention on other direct readouts of the Shh pathway that could be readily quantified. We observed a similar ventral expansion in the number of neuronal progenitors expressing Olig2 (*cSmo*: 125.8±12.9, n=5, versus control: 73.4±6.5, n=5, P<0.0001) and Ki67 (*cSmo*: 107.0±13.5, n=8, versus control: 81.8±16.4, n=9, P=0.0037) in *cSmo* embryos (Fig. 6B,C). The increased proliferation of ventral tuberal progenitors may explain why the ventricle is extended ventrally in *cSmo* embryos (Fig. 6A-E). Notably, the cells displaying ectopic expression of Nkx2.2, Olig2 and Ki67 were not GFP positive, suggesting that they had not undergone *Smo* recombination (Fig. S5). No change in the expression of *Gli1* was observed between *cSmo* and control embryos at E14.5 or earlier stages, suggesting that the ectopic response to Shh signaling was transient and/or below the sensitivity of this marker (Fig. 6D). The most parsimonious explanation for these results is that the conditional deletion of *Smo* prevented the normal uptake of Shh ligand, causing a non-cell autonomous gain in Shh signaling in neighboring wild-type cells (Fig. 6E).

DISCUSSION

Shh directs dorsoventral patterning and neurogenesis in the hypothalamus

Our results confirm that the early source of Shh in the anterior diencephalon is required for the formation of diverse neuronal cell types in the tuberal hypothalamus (Szabó et al., 2009; Shimogori et al., 2010; Zhao et al., 2012). To understand the mechanism underlying the loss of these cell types in $Shh^{\Delta hyp}$ mutants, we evaluated embryos at E10.5 and observed a failure in the activation of patterning, proliferation and neurogenic programs. This result is consistent with known morphogenetic roles of Shh in establishing ventral neuronal identities through the regulation of homeodomain and bHLH transcription factors with some notable differences described below (Ericson et al., 1997; Briscoe and Ericson, 1999; Briscoe et al., 2000; Muhr et al., 2001; Balaskas et al., 2012).

At spinal cord and hindbrain levels of the CNS, the notochord is the principal source of Shh required to specify ventral neuronal progenitors, whereas the secondary source of Shh in the floor plate

Development (2018) 145, dev167379. doi:10.1242/dev.167379

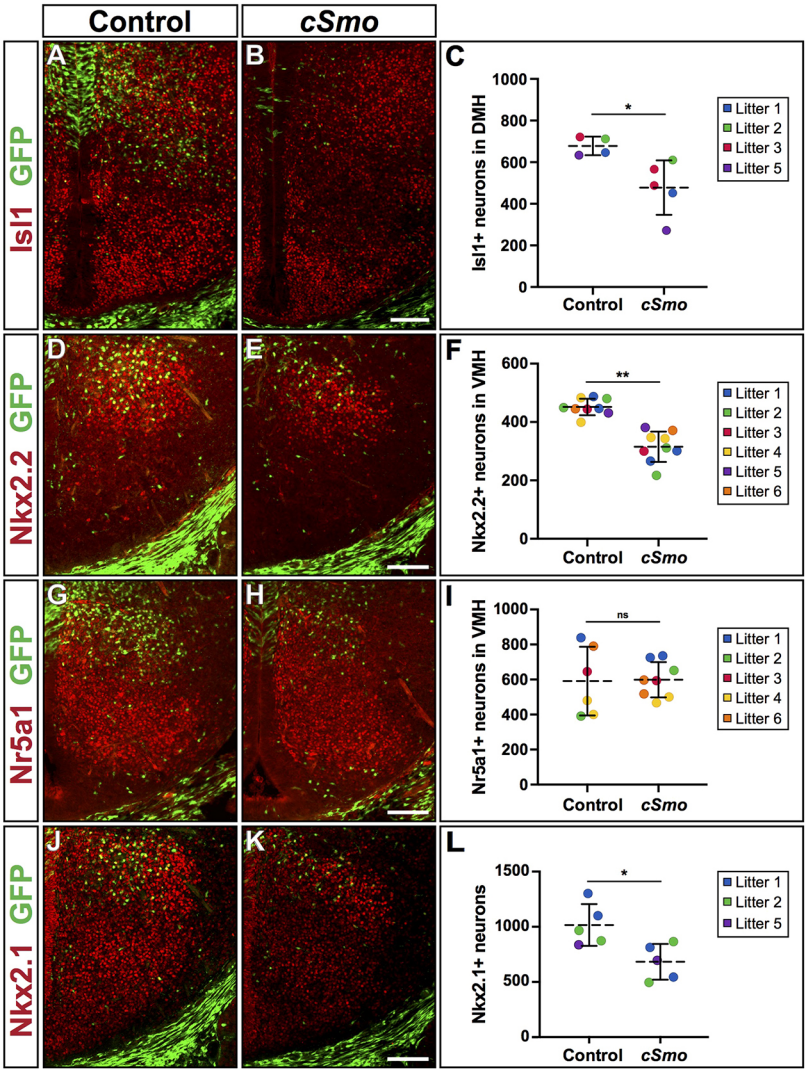

Fig. 5. Shh signaling is required for subtype identity of VMH and DMH neurons. Coronal sections through the tuberal hypothalamus of control and *cSmo* embryos at E14.5 that received tamoxifen at E10.5. (A-C) The number of cells expressing Isl1 in the DMH is reduced in *cSmo* embryos (control n=4, *cSmo* n=5, *P=0.0229). (D-F) The number of post-mitotic neurons expressing Nkx2.2 in the dorsal VMH is reduced in *cSmo* embryos compared with control littermates (n=9, **P<0.0001). (G-I) The number of VMH neurons expressing Nr5a1 is equivalent between control and *cSmo* embryos (control n=6, *cSmo* n=8, ns, P>0.05). (J-L) The number of postmitotic neurons expressing Nkx2.1 in the tuberal hypothalamus is reduced in *cSmo* embryos (n=5, *P=0.0174). For all graphs, horizontal dotted line represents the mean and error bars indicate s.d. Each data point represents the number of cells expressing a given marker on a single hemi-section at equivalent levels of the tuberal hypothalamus from a single embryo color-coded by litter (n=number of embryos analyzed). Statistical analysis was performed using a two-tailed unpaired t-test. Scale bars: 100 µm.

is needed for the formation of later-born glial and ependymal cells types (Matise et al., 1998; Yu et al., 2013). In contrast, expression of Shh in the prechordal plate is transient and only present for sufficient time to specify the hypothalamic territory, marked by Nkx2.1, but not the identity of neuronal progenitors (Szabó et al., 2009). Instead, it is the neuronal source of Shh in the hypothalamus that establishes ARC, VMH and DMH progenitor domains. Thus, whereas notochord-derived Shh activates target genes such as *Nkx2.2* and *Olig2* in the overlying neural tube, a similar function is fulfilled by the hypothalamic source of Shh. Given that hypothalamic neurons develop over a protracted period compared with most spinal cord neurons, it makes sense that they rely on an enduring source of Shh within the hypothalamus for their development (Davis et al., 2004; Altman and Bayer, 1986; Ishii and Bouret, 2012).

Shh restricts ventral midline development in the tuberal hypothalamus

In addition to the dorsoventral patterning and neurogenic defects in $Shh^{\Delta hyp}$ mutants, our analysis revealed an unexpected expansion of ventral midline territory. The increased number of ventral midline cells in $Shh^{\Delta hyp}$ embryos is likely a consequence of heightened Bmp signaling, as evidenced by the expanded zone of non-proliferation and *Tbx3* expression, two molecular readouts of this pathway (Manning et al., 2006). Indeed, loss of Shh signaling in the anterior hypothalamus of $Shh^{\Delta hyp}$ embryos was shown to cause a rostral shift in *Bmp4* expression as early as E9.5 (Zhao et al., 2012). A similar phenotype was also observed in $Lrp2^{-/-}$ mutant embryos, including downregulation of Shh signaling, a flattened and expanded ventral midline, and a rostral shift in *Bmp4* expression (Christ et al., 2012). Lrp2 belongs to the LDL receptor gene family and binds both Shh (as a co-receptor) and Bmp4 (as a scavenger receptor) (McCarthy et al., 2002; Spoelgen et al., 2005; Christ et al., 2012). Therefore, disruption in the balance of Shh and Bmp signaling, loss and gain respectively, is likely responsible for the ventral midline defects in $Lrp2^{-/-}$ and $Shh^{\Delta hyp}$ mutants.

The additional role that we uncovered for Shh in restricting ventral midline development in the tuberal hypothalamus is intriguing given the opposite function it plays in promoting floor-plate induction in posterior regions of the CNS (Echelard et al., 1993; Roelink et al., 1995; Martí et al., 1995; Ericson et al., 1996; Chiang et al., 1996). Why might Shh have contrasting roles in the development of ventral midline cells at different axial levels of the neural tube? First, ventral midline cells in the tuberal hypothalamus, known as the median eminence, differ from floor-plate cells in the spinal cord in that the former comprises tanycytes, a specialized type of radial glia with neurogenic and gliogenic properties (Rizzoti and Lovell-Badge, 2017). In mammals, floor-plate cells of the

Development (2018) 145, dev167379. doi:10.1242/dev.167379

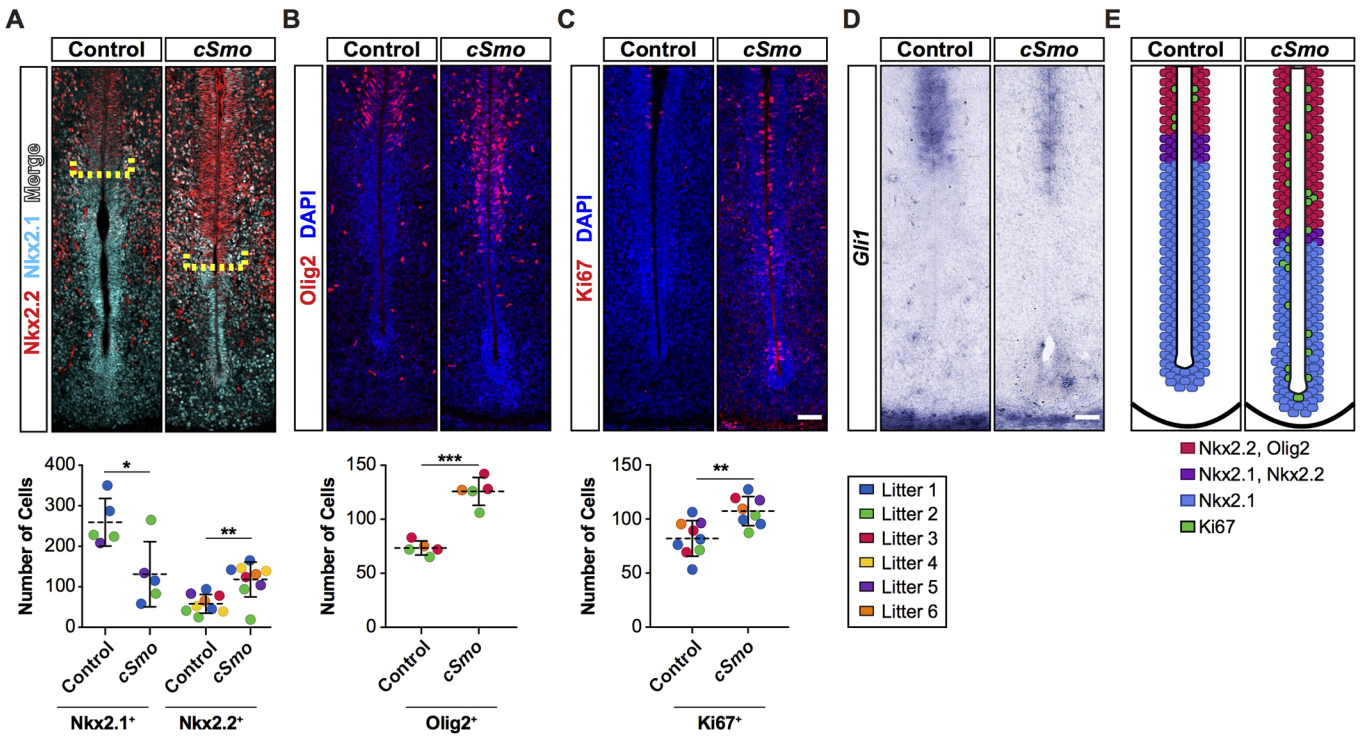

Fig. 6. Non-cell autonomous alterations in hypothalamic progenitors in *cSmo* embryos. Coronal sections through the tuberal hypothalamus of control and *cSmo* embryos at E14.5 (tamoxifen administered at E10.5). (A) The boundary between Nkx2.1- and Nk2.2-expressing progenitors (yellow bracket) is shifted ventrally in the ventricular zone of *cSmo* embryos compared with control littermates. Ventral expansion in the number of Nkx2.2-expressing progenitors (n=9, $^{**}P$=0.002) is concomitant with a reduction in the number of cells expressing Nkx2.1 (n=5, $^{*}P$=0.0205). (B) The number of Olig2-expressing progenitors is ventrally expanded in *cSmo* embryos compared with control littermates (n=5, $^{***}P$<0.0001). (C) The number of Ki67-expressing progenitors is ventrally expanded in *cSmo* embryos compared with control littermates (control n=9, *cSmo* n=8, $^{**}P$=0.0037). (D) *Gli1* expression is unchanged between control and *cSmo* embryos (n=3). (E) Schematic model depicting the non-cell autonomous gain in Shh responsiveness by ventral tuberal hypothalamic progenitors in *cSmo* mutant embryos compared with control littermates. For all graphs, horizontal dotted line represents the mean and error bars indicate s.d. Each data point represents the number of cells expressing a given marker on a single hemi-section at equivalent levels of the tuberal hypothalamus from a single embryo color-coded by litter (n=number of embryos analyzed). Statistical analysis was performed using a two-tailed unpaired *t*-test. Scale bars: 50 µm.

spinal cord are considered glial like but do not give rise to neurons or glia. Tanycytes are an integral component of the hypophyseal portal system that connects the hypothalamus to the pituitary gland and they regulate a variety of homeostatic processes owing to their access to blood-borne signals (Rodríguez et al., 2005; Robins et al., 2013; Bolborea and Dale, 2013). Second, the hypothalamic ventral midline is a site of integration for multiple signaling pathways, including Shh, Bmp, Wnt and Fgf, that help to facilitate the unique organization of the hypothalamic-pituitary axis (Manning et al., 2006; Davis and Camper, 2007; Zhu et al., 2007; Potok et al., 2008; Zhao et al., 2012; Carreno et al., 2017; Fu et al., 2017). At the level of the spinal cord, Shh is the primary regulator of ventral neuronal identities, with additional signals serving to modulate Shh responsiveness (Gouti et al., 2015; Kong et al., 2015). Third, Shh-expressing cells in the hypothalamus are different from elsewhere in the neural tube in that they constitute actively dividing neuronal progenitors (Szabó et al., 2009; this study). Within the spinal cord, Shh-expressing floor-plate cells lack neurogenic properties. Given the clear differences in ventral development between the hypothalamus and spinal cord, it is not altogether surprising that Shh exhibits unique and overlapping functions at each of these CNS regions.

Later Shh signaling: delineating fates

We sought to investigate roles and requirements for the enduring source of Shh in the tuberal hypothalamus after patterning is established. Though our lineage-tracing experiments only marked progenitors at a single time point (E10.5), we identified general contributions of these lineages to several hypothalamic nuclei. Our experiments revealed biased contributions of Shh-expressing and Shh-responding lineages to compartments of the VMH and DMH. On the basis of these observations, we wondered whether integration of progenitors may serve as a potential means by which neuronal heterogeneity is achieved within tuberal hypothalamic nuclei.

Shh-expressing and Shh-responsive populations mix to give rise to the large domain of Nr5a1 neurons in the VMH, although their contributions remain spatially segregated. Initially found broadly in the VMH, Nr5a1 expression becomes restricted to the VMH_{DM} by P0 (Cheung et al., 2013; Correa et al., 2015). Transcriptome analysis of the VMH in both neonatal and adult mice revealed enrichment of 200 genes relative to expression in neighboring nuclei (Segal et al., 2005; Kurrasch et al., 2007). Examining the patterns of these markers showed distinct spatial domains and biases, some overlapping with Nr5a1 and some mutually exclusive. Thus, it is clear that VMH neurons are diverse in nature. Molecular characterization of VMH neuronal subclasses has largely been performed in postnatal animals. Specifically, Islet1 and ERα are restricted to the VMH_{VL} (Davis et al., 2004), BDNF to the VMH_{DM} and VMH_{C} (McClellan et al., 2006), and the leptin receptor to the VMH_{DM} (Balthasar et al., 2004; Dhillon et al., 2006). However, little is known about the processes through which these diverse

Development (2018) 145, dev167379. doi:10.1242/dev.167379

populations are specified. Thus, within the VMH, the ventral bias of cells derived from Shh-expressing progenitors and the dorsal bias of Gli1-expressing descendants may indicate a role for Shh signaling in delineating distinct neuronal fates within a single nucleus.

The migration of a small number of Shh-responsive progenitors into the VMH bears similarity to other hypothalamic cell types that originate from outside of their local progenitor territory. Most neuronal populations in the ARC are generated from multipotent progenitors that migrate radially from the adjacent ventricular zone (Li et al., 1996; McNay et al., 2006; Yee et al., 2009; Pelling et al., 2011; Lu et al., 2013; Lee et al., 2016). However, some cells migrate tangentially from distal locations. For example, GnRH neurons originate in the olfactory bulb and navigate substantial distance to access their final location within the ARC (Wray et al., 1989; Wray, 2002). Moreover, gene expression studies suggest that some Sst neurons migrate to the ARC from an anterior hypothalamic birthplace (Morales-Delgado et al., 2011). We propose that the migration of a Shh-responsive cell population into the VMH, albeit from a nearby location, may further explain how cellular diversity is achieved in this nucleus.

Later Shh signaling: maintaining proliferation of progenitor pools

In assessing the requirements of Shh signaling at later stages of hypothalamic development, we observed a dependency on Smo for maintaining tuberal hypothalamic progenitors in a mitotically active state during peak periods of VMH and DMH neurogenesis. Consequently, the contribution of Shh-responsive progenitors to the VMH and DMH was reduced in *cSmo* embryos, resulting in a 30% reduction in the number of Nkx2.2- and Isl1-expressing neurons, respectively. These results are consistent with previous findings demonstrating a mitogenic role for Shh in other neurodevelopmental contexts (Rowitch et al., 1999; Wallace, 1999; Wechsler-Reya and Scott, 1999; Fuccillo et al., 2006; Komada et al., 2008).

Non-cell-autonomous phenotypes in *cSmo* mutants due to ectopic Shh signaling

The *cSmo* mutants used in our study show a cell-autonomous loss of Shh signaling. In addition to its role as Shh receptor, Ptch1 also functions to sequester Shh in a feedback mechanism that limits the spread of Shh ligand in a field of receptive cells (Jeong and McMahon, 2005). In $Smo^{-/-}$ embryos, there is less Shh uptake and a greater distribution of Shh ligand due to lower amounts of Ptch1 on the cell surface (Chamberlain et al., 2008). In our *cSmo* mutants, neighboring control cells that have not undergone Smo recombination gain responsiveness to residual Shh ligand and ectopically activate several targets of Shh signaling (Nkx2.2, Olig2 and Ki67) in the ventricular zone of the ventral tuberal hypothalamus. A similar non-cell-autonomous gain in Shh signaling was previously described in response to mosaic deletion of Smo in the ventral telencephalon (Xu et al., 2010).

Our observation of increased Shh signaling in non-recombined cells from *cSmo* mutant embryos is provocative in light of the association of somatic mutations in regulators of Shh signaling with hypothalamic hamartomas (Craig et al., 2008; Wallace et al., 2008; Hildebrand et al., 2016; Saitsu et al., 2016). Hypothalamic hamartomas are benign tumors that form during fetal brain development and, depending on their size and location, may disrupt endocrine function and cause seizures. Dominant mutations in *GLI3* that produce a truncated protein with constitutive repressor activity have been identified in hypothalamic hamartomas (Craig et al., 2008; Wallace et al., 2008; Hildebrand et al., 2016; Saitsu et al., 2016). Mutations in other components of the SHH signaling pathway, *OFD1* and *PRKACA* (which encodes the catalytic subunit α of PKA), have also been described in resected hamartoma tissue (Hildebrand et al., 2016; Saitsu et al., 2016).

The mechanism of hypothalamic hamartoma formation is unknown; however, several key features of their biology may reveal important insight into their development. First, the truncated form of GLI3 acts as a dominant repressor of Shh signaling. Second, most hamartomas are mosaic with varying amounts of mutant and wild-type cells (Saitsu et al., 2016). Third, GLI3 mutant cells cause a cell-autonomous reduction in SHH signaling that possibly manifests in reduced PTCH1 expression and increased dissemination of SHH ligand. Finally, accumulation of extracellular SHH is predicted to induce ectopic signaling in neighboring wild-type cells, resulting in a transient growth advantage.

In cases of Pallister Hall syndrome, germline-truncating mutations in *GLI3* cause a reduction, but not complete blockade, of SHH signaling in all cells (Kang et al., 1997; Böse et al., 2002). Hypothalamic hamartomas may form in response to stochastic upregulation of SHH signaling within a single cell or cluster of cells. A higher concentration of SHH may be required for hamartoma formation in cases of Pallister Hall syndrome to overcome the negative influence of the truncating *GLI3* mutation on pathway activation.

Hypothalamic hamartomas are also associated with SOX2 haploinsufficiency in humans (Kelberman et al., 2006). Similar hypothalamic protuberances have been described in mouse embryos with hypomorphic *Sox2* mutations (Langer et al., 2012). Interestingly, these $Sox2^{hyp}$ mutants show a dramatic decrease in *Gli3* expression in the ventral midline of the tuberal hypothalamus, and ectopic *Shh* transcription. As *Gli3* mutant mice do not exhibit hypothalamic hamartomas, it is conceivable that the gain in Shh expression contributes to the phenotype, which is consistent with our model. Although experiments in our study did not extend into postnatal life and may not have targeted enough cells to induce hypothalamic hamartomas, they do nevertheless offer a compelling explanation for how these ectopic growths might form during brain development.

MATERIALS AND METHODS

Mice

All animal work was approved by the Institutional Animal Care and Use Committee (IACUC) at the Perelman School of Medicine, University of Pennsylvania. The *SBE2-cre* mouse line has been previously described (Zhao et al., 2012). $Gli1^{CreER}$ ($Gli1^{tm3(cre/ERT2)Alj}$), $Gli1^{lacZ}$ ($Gli1^{tm2Alj}$), $Rosa^{ZsGreen}$ ($Gt(ROSA)26Sor^{tm6(CAG-ZsGreen1)Hze}$), $Shh^{+/-}$, $Shh^{loxp/loxp}$ (Shh^{tm2Amc}), Shh^{CreER} ($Shh^{tm2(cre/ERT2)Cjt}$), $Smo^{+/-}$ (Smo^{tm1Amc}) and $Smo^{loxp/loxp}$ (Smo^{tm2Amc}) mouse strains were procured from the Jackson Laboratories. Tamoxifen dissolved in corn oil was orally gavaged at 0.15 mg/g body weight to pregnant dams at appropriate developmental time points.

Tissue dissection

Embryos were collected at the stated developmental age, with noon of plug day designated E0.5. Heads were dissected in ice-cold PBS and fixed in 4% paraformaldehyde (PFA) for 90 min to overnight at 4°C. Heads were then cryoprotected in 30% sucrose and embedded in Tissue-Tek OCT compound. Frozen tissue was cryosectioned at 16 µm (for E12.5 and E13.5 embryos), 18 µm (for E14.5 embryos) or 20 µm (for E10.5 and E18.5 embryos).

Immunohistochemistry and section *in situ* hybridization

Immunohistochemistry was performed with the following antibodies: mouse anti-Ascl1 (1:100 BD Pharmingen, 556604), rabbit anti-cleaved

Development (2018) 145, dev167379. doi:10.1242/dev.167379

caspase 3 (1:1000, Cell Signaling, 9661), mouse anti-Gad1 (1:500, EMD Millipore, MAB5406), mouse anti-Isl1 (1:100, DSHB, 39.4D5), rabbit anti-Ki67 (1:1000, Novocastra. NCL-Ki67p), rabbit anti-Nkx2.1 (1:1000, Abcam, AB76013), mouse anti-Nkx2.2 (1:1000, DSHB, 74.5A5), rabbit anti-Olig2 (1:500, Millipore, AB9610), mouse anti-Pax6 (1:1000, DSHB, Pax6), rabbit anti-POMC (1:500, Phoenix Pharmaceuticals, H-029-30), mouse anti-Nr5a1 (1:200, R&D Systems, PP-N1665), rat anti-somatostatin (1:200, Millipore, MAB354) rabbit anti-tyrosine hydroxlase (1:1000, Pel-Freez, P40101-0). Somatostatin, Pax6, Nkx2.2, Nr5a1, Gad1 and Isl1 antibodies required antigen retrieval in 10 mM citric acid buffer (pH 6.0) at 90°C. A Mouse on Mouse detection kit (Vector Laboratories BMK-2202) was used for blocking and primary antibody dilution of Nkx2.2, Gad1 and Isl1 antibodies.

Detection of primary antibodies was achieved using secondary antibodies conjugated to Cy3 anti-rabbit (1:200, 111-165-003, Jackson ImmunoResearch Laboratories), Cy3 anti-mouse (1:200, 115-166-006, Jackson ImmunoResearch Laboratories), Cy3 anti-rat (1:200, 112-166-003, Jackson ImmunoResearch Laboratories) or AlexaFluor 633 anti-rabbit (1:100, Invitrogen, A21070). Section *in situ* hybridization with digoxygenin-UTP-labeled riboprobes was performed as described previously (Nissim et al., 2007). A minimum of three embryos per genotype was evaluated with each antibody or *in situ* probe.

β-Galactosidase staining

Heads from *Gli1*$^{lacZ/+}$ embryos were dissected in ice-cold PBS and fixed in 4% PFA for 90 min at 4°C. Heads were then cryoprotected in 30% sucrose and embedded in Tissue-Tek OCT compound. Frozen tissue was cryosectioned at 20 µm. Slides were then stained in a solution containing 1 mg/ml X-gal at 37°C overnight. Following staining, slides were post-fixed in 4% PFA and washed in PBS.

Alignment of sections, quantification and statistical analysis

All cell counts were performed using the cell counter function in ImageJ (NIH) on hemi- or full tissue sections from at least three control and mutant embryos. To ensure that all quantifications were performed at similar axial levels, we performed Nr5a1 immunostaining to denote the rostral and caudal limits of the VMH. Fate-mapping and gene expression studies were performed at the midpoint of the VMH territory.

In cases where double labeling was examined for GFP and another cell-specific marker, the tissue was imaged in a single *z*-plane. Each channel (green for GFP, red for the marker) was first examined independently, assigning a positive count for a given marker to the DAPI-stained nucleus most closely associated with the staining. A cell was only counted as double labeled if a single nucleus marked by DAPI had been assigned to the cell labeled by GFP and the cell-specific marker. Statistical analysis of all cell counts was performed in GraphPad Prism using the Student's *t*-test.

Acknowledgements

We thank Ishmail Abdus-Saboor, Sarah Millar and Alex Rohacek for critical comments on the manuscript. We appreciate use of antibodies obtained from the Developmental Studies Hybridoma Bank, created by the NICHD of the NIH and maintained at The University of Iowa, Department of Biology, Iowa City, IA 52242.

Competing interests

The authors declare no competing or financial interests.

Author contributions

Conceptualization: D.J.E., T.S.C., S.E.B.; Methodology: D.J.E., T.S.C.; Formal analysis: D.J.E., T.S.C.; Investigation: T.S.C., S.E.B.; Resources: D.J.E.; Writing - original draft: D.J.E., T.S.C.; Writing - review & editing: S.E.B.; Supervision: D.J.E.; Funding acquisition: D.J.E.

Funding

This work was supported by a grant from the National Institutes of Health (R01 NS039421) to D.J.E. Deposited in PMC for release after 12 months.

Supplementary information

Supplementary information available online at
http://dev.biologists.org/lookup/doi/10.1242/dev.167379.supplemental

References

Altman, J. and Bayer, S. A. (1986). The development of the rat hypothalamus. *Adv. Anat. Embryol. Cell Biol.* **100**, 1-178.

Alvarez-Bolado, G., Paul, F. A. and Blaess, S. (2012). Sonic hedgehog lineage in the mouse hypothalamus: from progenitor domains to hypothalamic regions. *Neural Dev.* **7**, 4.

Balaskas, N., Ribeiro, A., Panovska, J., Dessaud, E., Sasai, N., Page, K. M., Briscoe, J. and Ribes, V. (2012). Gene regulatory logic for reading the Sonic Hedgehog signaling gradient in the vertebrate neural tube. *Cell* **148**, 273-284.

Balthasar, N., Coppari, R., McMinn, J., Liu, S. M., Lee, C. E., Tang, V., Kenny, C. D., McGovern, R. A., Chua, S. C., Elmquist, J. K. et al. (2004). Leptin receptor signaling in POMC neurons is required for normal body weight homeostasis. *Neuron* **42**, 983-991.

Bedont, J. L., Newman, E. A. and Blackshaw, S. (2015). Patterning, specification, and differentiation in the developing hypothalamus. *Wiley Interdiscip. Rev. Dev. Biol.* **4**, 445-468.

Bolborea, M. and Dale, N. (2013). Hypothalamic tanycytes: potential roles in the control of feeding and energy balance. *Trends Neurosci.* **36**, 91-100.

Böse, J., Grotewold, L. and Rüther, U. (2002). Pallister–Hall syndrome phenotype in mice mutant for Gli3. *Hum. Mol. Genet.* **11**, 1129-1135.

Briscoe, J. and Ericson, J. (1999). The specification of neuronal identity by graded Sonic Hedgehog signalling. *Semin. Cell Dev. Biol.* **10**, 353-362.

Briscoe, J., Pierani, A., Jessell, T. M. and Ericson, J. (2000). A homeodomain protein code specifies progenitor cell identity and neuronal fate in the ventral neural tube. *Cell* **101**, 435-445.

Büdefeld, T., Tobet, S. A. and Majdic, G. (2011). Altered position of cell bodies and fibers in the ventromedial region in SF-1 knockout mice. *Exp. Neurol.* **232**, 176-184.

Burbridge, S., Stewart, I. and Placzek, M. (2016). Development of the neuroendocrine hypothalamus. *Compr. Physiol.* **6**, 623-643.

Carreno, G., Apps, J. R., Lodge, E. J., Panousopoulos, L., Haston, S., Gonzalez-Meljem, J. M., Hahn, H., Andoniadou, C. L. and Martinez-Barbera, J. P. (2017). Hypothalamic sonic hedgehog is required for cell specification and proliferation of LHX3/LHX4 pituitary embryonic precursors. *Development* **144**, 3289-3302.

Chamberlain, C. E., Jeong, J.,Guo, C., Allen, B. L. and McMahon, A. P. (2008). Notochord-derived Shh concentrates in close association with the apically positioned basal body in neural target cells and forms a dynamic gradient during neural patterning. *Development* **135**, 1097-1106.

Cheung, C. C., Kurrasch, D. M., Liang, J. K. and Ingraham, H. A. (2013). Genetic labeling of steroidogenic factor-1 (SF-1) neurons in mice reveals ventromedial nucleus of the hypothalamus (VMH) circuitry beginning at neurogenesis and development of a separate non-SF-1 neuronal cluster in the ventrolateral VMH. *J. Comp. Neurol.* **521**, 1268-1288.

Chiang, C., Litingtung, Y., Lee, E., Young, K. E., Corden, J. L., Westphal, H. and Beachy, P. A. (1996). Cyclopia and defective axial patterning in mice lacking Sonic hedgehog gene function. *Nature* **383**, 407-413.

Christ, A., Christa, A., Kur, E., Lioubinski, O., Bachmann, S., Willnow, T. E. and Hammes, A. (2012). LRP2 is an auxiliary SHH receptor required to condition the forebrain ventral midline for inductive signals. *Dev. Cell* **22**, 268-278.

Correa, S. M., Newstrom, D. W., Warne, J. P., Flandin, P., Cheung, C. C., Lin-Moore, A. T., Pierce, A. A., Xu, A. W., Rubenstein, J. L. and Ingraham, H. A. (2015). An estrogen-responsive module in the ventromedial hypothalamus selectively drives sex-specific activity in females. *Cell Rep.* **10**, 62-74.

Craig, D. W., Itty, A., Panganiban, C., Szelinger, S., Kruer, M. C., Sekar, A., Reiman, D., Narayanan, V., Stephan, D. A. and Kerrigan, J. F. (2008). Identification of somatic chromosomal abnormalities in hypothalamic hamartoma tissue at the GLI3 locus. *Am. J. Hum. Genet.* **82**, 366-374.

Dale, J. K., Vesque, C., Lints, T. J., Sampath, T. K., Furley, A., Dodd, J. and Placzek, M. (1997). Cooperation of BMP7 and SHH in the induction of forebrain ventral midline cells by prechordal mesoderm. *Cell* **90**, 257-269.

Davis, S. W. and Camper, S. A. (2007). Noggin regulates Bmp4 activity during pituitary induction. *Dev. Biol.* **305**, 145-160.

Davis, A. M., Seney, M. L., Stallings, N. R., Zhao, L., Parker, K. L. and Tobet, S. A. (2004). Loss of steroidogenic factor 1 alters cellular topography in the mouse ventromedial nucleus of the hypothalamus. *J. Neurobiol.* **60**, 424-436.

Dhillon, H., Zigman, J. M., Ye, C., Lee, C. E., McGovern, R. A., Tang, V., Kenny, C. D., Christiansen, L. M., White, R. D., Edelstein, E. A. et al. (2006). Leptin directly activates SF1 neurons in the VMH, and this action by leptin is required for normal body-weight homeostasis. *Neuron* **49**, 191-203.

Echelard, Y., Epstein, D. J., St-Jacques, B., Shen, L., Mohler, J., McMahon, J. A. and McMahon, A. P. (1993). Sonic hedgehog, a member of a family of putative signaling molecules, is implicated in the regulation of CNS polarity. *Cell* **75**, 1417-1430.

Ericson, J., Morton, S., Kawakami, A., Roelink, H. and Jessell, T. M. (1996). Two critical periods of Sonic Hedgehog signaling required for the specification of motor neuron identity. *Cell* **87**, 661-673.

Ericson, J., Rashbass, P., Schedl, A., Brenner-Morton, S., Kawakami, A., van Heyningen, V., Jessell, T. M. and Briscoe, J. (1997). Pax6 controls progenitor

cell identity and neuronal fate in response to graded Shh signaling. *Cell* **90**, 169-180.
Fu, T., Towers, M. and Placzek, M. A. (2017). Fgf10+ progenitors give rise to the chick hypothalamus by rostral and caudal growth and differentiation. *Development* **144**, 3278-3288.
Fuccillo, M., Joyner, A. L. and Fishell, G. (2006). Morphogen to mitogen: the multiple roles of hedgehog signalling in vertebrate neural development. *Nat. Rev. Neurosci.* **7**, 772-783.
Gouti, M., Metzis, V. and Briscoe, J. (2015). The route to spinal cord cell types: a tale of signals and switches. *Trends Genet.* **31**, 282-289.
Hashikawa, Y., Hashikawa, K., Falkner, A. L. and Lin, D. (2017). Ventromedial hypothalamus and the generation of aggression. *Front. Syst. Neurosci.* **11**, 1-13.
Hildebrand, M. S., Griffin, N. G., Damiano, J. A., Cops, E. J., Burgess, R., Ozturk, E., Jones, N. C., Leventer, R. J., Freeman, J. L., Harvey, A. S. et al. (2016). Mutations of the Sonic hedgehog pathway underlie hypothalamic Hamartoma with Gelastic epilepsy. *Am. J. Hum. Genet.* **99**, 423-429.
Ikeda, Y., Luo, X., Abbud, R., Nilson, J. H. and Parker, K. L. (1995). The nuclear receptor steroidogenic factor 1 is essential for the formation of the ventromedial hypothalamic nucleus. *Mol. Endocrinol.* **9**, 478-486.
Ishii, Y. and Bouret, S. G. (2012). Embryonic birthdate of hypothalamic leptin-activated neurons in mice. *Endocrinology* **153**, 3657-3667.
Jeong, J. L. and McMahon, A. P. (2005). Growth and pattern of the mammalian neural tube are governed by partially overlapping feedback activities of the hedgehog antagonists patched 1 and Hhip1. *Development* **132**, 143-154.
Kang, S., Graham, J. M. Jr, Olney, A. H. and Biesecker, L. G. (1997). GLI3 frameshift mutations cause autosomal dominant Pallister-Hall syndrome. *Nat. Genet.* **15**, 266-268.
Kelberman, D., Rizzoti, K., Avilion, A., Bitner-Glindzicz, M., Cianfarani, S., Collins, J., Chong, W. K., Kirk, J. M., Achermann, J. C., Ross, R. et al. (2006). Mutations within Sox2/SOX2 are associated with abnormalities in the hypothalamo-pituitary-gonadal axis in mice and humans. *J. Clin. Invest.* **116**, 2442-2455.
Kim, K. W., Li, S., Zhao, H., Peng, B., Tobet, S. A., Elmquist, J. K., Parker, K. L. and Zhao, L. (2010). CNS-specific ablation of steroidogenic factor 1 results in impaired female reproductive function. *Mol. Endocrinol.* **24**, 1240-1250.
Kimura, S., Hara, Y., Pineau, T., Fernandez-Salguero, P., Fox, C. H., Ward, J. M. and Gonzalez, F. J. (1996). The T/ebp null mouse: thyroid-specific enhancer-binding protein is essential for the organogenesis of the thyroid, lung, ventral forebrain, and pituitary. *Genes Dev.* **10**, 60-69.
Klöckener, T., Hess, S., Belgardt, B. F., Paeger, L., Verhagen, L. A. W., Husch, A., Sohn, J.-W., Hampel, B., Dhillon, H., Zigman, J. M. et al. (2011). High-fat feeding promotes obesity via insulin receptor/PI3K-dependent inhibition of SF-1 VMH neurons. *Nat. Neurosci.* **14**, 911-918.
Komada, M., Saitsu, H., Kinboshi, M., Miura, T., Shiota, K. and Ishibashi, M. (2008). Hedgehog signaling is involved in development of the neocortex. *Development* **135**, 2717-2727.
Kong, J. H., Yang, L., Dessaud, E., Chuang, K., Moore, D. M., Rohatgi, R., Briscoe, J. and Novitch, B. G. (2015). Notch activity modulates the responsiveness of neural progenitors to sonic hedgehog signaling. *Dev. Cell* **33**, 373-387.
Kunwar, P. S., Zelikowsky, M., Remedios, R., Cai, H., Yilmaz, M., Meister, M. and Anderson, D. J. (2015). Ventromedial hypothalamic neurons control a defensive emotion state. *eLife* **4**, e06633.
Kurrasch, D. M., Cheung, C. C., Lee, F. Y., Tran, P. V., Hata, K. and Ingraham, H. A. (2007). The neonatal ventromedial hypothalamus transcriptome reveals novel markers with spatially distinct patterning. *J. Neurosci.* **27**, 13624-13634.
Langer, L., Taranova, O., Sulik, K. and Pevny, L. (2012). SOX2 hypomorphism disrupts development of the prechordal floor and optic cup. *Mech. Dev.* **129**, 1-12.
Lee, H., Kim, D.-W., Remedios, R., Anthony, T. E., Chang, A., Madisen, L., Zeng, H. and Anderson, D. J. (2014). Scalable control of mounting and attack by Esr1+ neurons in the ventromedial hypothalamus. *Nature* **509**, 627-632.
Lee, B., Lee, S., Lee, S.-K. and Lee, J. W. (2016). The LIM-homeobox transcription factor Isl1 plays crucial roles in the development of multiple arcuate nucleus neurons. *Development* **143**, 3763-3773.
Lei, Q., Jeong, Y., Misra, K., Li, S., Zelman, A. K., Epstein, D. J. and Matise, M. P. (2006). Wnt signaling inhibitors regulate the transcriptional response to morphogenetic Shh-Gli signaling in the neural tube. *Dev. Cell* **11**, 325-337.
Li, H., Zeitler, P. S., Valerius, M. T., Small, K. and Potter, S. S. (1996). Gsh-1, an orphan Hox gene, is required for normal pituitary development. *EMBO J.* **15**, 714-724.
Lin, D., Boyle, M. P., Dollar, P., Lee, H., Lein, E. S., Perona, P. and Anderson, D. J. (2011). Functional identification of an aggression locus in the mouse hypothalamus. *Nature* **470**, 221-226.
Lu, F., Kar, D., Gruenig, N., Zhang, Z. W., Cousins, N., Rodgers, H. M., Swindell, E. C., Jamrich, M., Schuurmans, C., Mathers, P. H. et al. (2013). Rax is a selector gene for mediobasal hypothalamic cell types. *J. Neurosci.* **33**, 259-272.
Majdic, G., Young, M., Gomez-Sanchez, E., Anderson, P., Szczepaniak, L. S., Dobbins, R. L., McGarry, J. D. and Parker, K. L. (2002). Knockout mice lacking steroidogenic factor 1 are a novel genetic model of hypothalamic obesity. *Endocrinology* **143**, 607-614.
Manning, L., Ohyama, K., Saeger, B., Hatano, O., Wilson, S. A., Logan, M. and Placzek, M. (2006). Regional morphogenesis in the hypothalamus: a BMP-Tbx2 pathway coordinates fate and proliferation through Shh downregulation. *Dev. Cell* **11**, 873-885.
Martí, E., Bumcrot, D. A., Takada, R. and McMahon, A. P. (1995). Requirement of 19K form of Sonic hedgehog for induction of distinct ventral cell types in CNS explants. *Nature* **375**, 322-325.
Matise, M. P., Epstein, D. J., Park, H. L., Platt, K. A. and Joyner, A. L. (1998). Gli2 is required for induction of floor plate and adjacent cells, but not most ventral neurons in the mouse central nervous system. *Development* **125**, 2759-2770.
McCarthy, R. A., Barth, J. L., Chintalapudi, M. R., Knaak, C. and Argraves, W. S. (2002). Megalin functions as an endocytic sonic hedgehog receptor. *J. Biol. Chem.* **277**, 25660-25667.
McClellan, K., Parker, K. and Tobet, S. (2006). Development of the ventromedial nucleus of the hypothalamus. *Front. Neuroendocrinol.* **27**, 193-209.
McNay, D. E. G., Pelling, M., Claxton, S., Guillemot, F. and Ang, S.-L. (2006). Mash1 is required for generic and subtype differentiation of hypothalamic neuroendocrine cells. *Mol. Endocrinol.* **20**, 1623-1632.
Morales-Delgado, N., Merchan, P., Bardet, S. M., Ferrán, J. L., Puelles, L. and Díaz, C. (2011). Topography of somatostatin gene expression relative to molecular progenitor domains during ontogeny of the mouse hypothalamus. *Front. Neuroanat.* **5**, 1-15.
Muhr, J., Andersson, E., Persson, M., Jessell, T. M. and Ericson, J. (2001). Groucho-mediated transcriptional repression establishes progenitor cell pattern and neuronal fate in the ventral neural tube. *Cell* **104**, 861-873.
Nissim, S., Allard, P., Bandyopadhyay, A., Harfe, B. D. and Tabin, C. J. (2007). Characterization of a novel ectodermal signaling center regulating Tbx2 and Shh in the vertebrate limb. *Dev. Biol.* **304**, 9-21.
Ohyama, K., Das, R. and Placzek, M. (2008). Temporal progression of hypothalamic patterning by a dual action of BMP. *Development* **135**, 3325-3331.
Pelling, M., Anthwal, N., McNay, D., Gradwohl, G., Leiter, A. B., Guillemot, F. and Ang, S.-L. (2011). Differential requirements for neurogenin 3 in the development of POMC and NPY neurons in the hypothalamus. *Dev. Biol.* **349**, 406-416.
Potok, M. A., Cha, K. B., Hunt, A., Brinkmeier, M. L., Leitges, M., Kispert, A. and Camper, S. A. (2008). WNT signaling affects gene expression in the ventral diencephalon and pituitary gland growth. *Dev. Dyn.* **237**, 1006-1020.
Rizzoti, K. and Lovell-Badge, R. (2017). Pivotal role of median eminence tanycytes for hypothalamic function and neurogenesis. *Mol. Cell. Endocrinol.* **445**, 7-13.
Robins, S. C., Stewart, I., McNay, D. E., Taylor, V., Giachino, C., Goetz, M., Ninkovic, J., Briancon, N., Maratos-Flier, E., Flier, J. S. et al. (2013). α-Tanycytes of the adult hypothalamic third ventricle include distinct populations of FGF-responsive neural progenitors. *Nat. Commun.* **4**, 2049.
Rodríguez, E. M., Blázquez, J. L., Pastor, F. E., Peláez, B., Peña, P., Peruzzo, B. and Amat, P. (2005). Hypothalamic tanycytes: a key component of brain-endocrine interaction. *Int. Rev. Cytol.* **247**, 89-164.
Roelink, H., Augsburger, A., Heemskerk, J., Korzh, V., Norlin, S., Ruiz i Altaba, A., Tanabe, Y., Placzek, M., Edlund, T. and Jessell, T. M. (1994). Floor plate and motor neuron induction by vhh-1, a vertebrate homolog of hedgehog expressed by the notochord. *Cell* **76**, 761-775.
Roelink, H., Porter, J. A., Chiang, C., Tanabe, Y., Chang, D. T., Beachy, P. A. and Jessell, T. M. (1995). Floor plate and motor neuron induction by different concentrations of the amino-terminal cleavage product of sonic hedgehog autoproteolysis. *Cell* **81**, 445-455.
Rowitch, D. H., S-Jacques, B., Lee, S. M. K., Flax, J. D., Snyder, E. Y. and McMahon, A. P. (1999). Sonic hedgehog regulates proliferation and inhibits differentiation of CNS precursor cells. *J. Neurosci.* **19**, 8954-8965.
Saitsu, H., Sonoda, M., Higashijima, T., Shirozu, H., Masuda, H., Tohyama, J., Kato, M., Nakashima, M., Tsurusaki, Y., Mizuguchi, T. et al. (2016). Somatic mutations in GLI3 and OFD1 involved in sonic hedgehog signaling cause hypothalamic hamartoma. *Ann Clin Transl Neurol* **3**, 356-365.
Saper, C. B. and Lowell, B. B. (2014). The hypothalamus. *Curr. Biol.* **24**, R1111-R1116.
Segal, J. P., Stallings, N. R., Lee, C. E., Zhao, L., Socci, N., Viale, A., Harris, T. M., Soares, M. B., Childs, G., Elmquist, J. K. et al. (2005). Use of laser-capture microdissection for the identification of marker genes for the ventromedial hypothalamic nucleus. *J. Neurosci.* **25**, 4181-4188.
Shimada, M. and Nakamura, T. (1973). Time of neuron origin in mouse hypothalamic nuclei. *Exp. Neurol.* **41**, 163-173.
Shimogori, T., Lee, D. A., Miranda-Angulo, A., Yang, Y., Wang, H., Jiang, L., Yoshida, A. C., Kataoka, A., Mashiko, H., Avetisyan, M. et al. (2010). A genomic atlas of mouse hypothalamic development. *Nat. Neurosci.* **13**, 767-775.
Silva, B. A., Mattucci, C., Krzywkowski, P., Murana, E., Illarionova, A., Grinevich, V., Canteras, N. S., Ragozzino, D. and Gross, C. T. (2013). Independent hypothalamic circuits for social and predator fear. *Nat. Neurosci.* **16**, 1731-1733.
Spoelgen, R., Hammes, A., Anzenberger, U., Zechner, D., Andersen, O. M., Jerchow, B. and Willnow, T. E. (2005). LRP2/megalin is required for patterning of the ventral telencephalon. *Development* **132**, 405-414.

Sussel, L., Marin, O., Kimura, S. and Rubenstein, J. L. (1999). Loss of Nkx2.1 homeobox gene function results in a ventral to dorsal molecular respecification within the basal telencephalon: evidence for a transformation of the pallidum into the striatum. *Development* **126**, 3359-3370.

Szabó, N.-E., Zhao, T., Çankaya, M., Theil, T., Zhou, X. and Alvarez-Bolado, G. (2009). Role of neuroepithelial Sonic hedgehog in hypothalamic patterning. *J. Neurosci.* **29**, 6989.

Tan, C. L. and Knight, Z. A. (2018). Regulation of body temperature by the nervous system. *Neuron* **98**, 31-48.

Tran, P. V., Lee, M. B., Marín, O., Xu, B., Jones, K. R., Reichardt, L. F., Rubenstein, J. R. and Ingraham, H. A. (2003). Requirement of the orphan nuclear receptor SF-1 in terminal differentiation of ventromedial hypothalamic neurons. *Mol. Cell. Neurosci.* **22**, 441-453.

Trowe, M.-O., Zhao, L., Weiss, A.-C., Christoffels, V., Epstein, D. J. and Kispert, A. (2013). Inhibition of Sox2-dependent activation of Shh in the ventral diencephalon by Tbx3 is required for formation of the neurohypophysis. *Development* **140**, 2299-2309.

Vokes, S. A., Ji, H., McCuine, S., Tenzen, T., Giles, S., Zhong, S., Longabaugh, W. J. R., Davidson, E. H., Wong, W. H. and McMahon, A. P. (2007). Genomic characterization of Gli-activator targets in sonic hedgehog-mediated neural patterning. *Development* **134**, 1977-1989.

Wallace, V. A. (1999). Purkinje-cell-derived Sonic hedgehog regulates granule neuron precursor cell proliferation in the developing mouse cerebellum. *Curr. Biol.* **9**, 445-448.

Wallace, R. H., Freeman, J. L., Shouri, M. R., Izzillo, P. A., Rosenfeld, J. V., Mulley, J. C., Harvey, A. S. and Berkovic, S. F. (2008). Somatic mutations in GLI3 can cause hypothalamic hamartoma and gelastic seizures. *Neurology* **70**, 653-655.

Wechsler-Reya, R. J. and Scott, M. P. (1999). Control of neuronal precursor proliferation in the cerebellum by Sonic Hedgehog. *Neuron* **22**, 103-114.

Wray, S. (2002). Development of gonadotropin-releasing hormone-1 neurons. *Front. Neuroendocrinol.* **23**, 292-316.

Wray, S., Grant, P. and Gainer, H. (1989). Evidence that cells expressing luteinizing hormone-releasing hormone mRNA in the mouse are derived from progenitor cells in the olfactory placode. *Proc. Natl. Acad. Sci. USA* **86**, 8132-8136.

Xie, Y. and Dorsky, R. I. (2017). Development of the hypothalamus: conservation, modification and innovation. *Development* **144**, 1588-1599.

Xu, Q., Guo, L., Moore, H., Waclaw, R. R., Campbell, K. and Anderson, S. A. (2010). Sonic Hedgehog signaling confers ventral telencephalic progenitors with distinct cortical interneuron fates. *Neuron* **65**, 328-340.

Yee, C. L., Wang, Y., Anderson, S., Ekker, M. and Rubenstein, J. L. R. (2009). Arcuate nucleus expression of NKX2.1 and DLX and lineages expressing these transcription factors in neuropeptide Y(+), proopiomelanocortin(+), and tyrosine hydroxylase(+) neurons in neonatal and adult mice. *J. Comp. Neurol.* **517**, 37-50.

Yu, K., McGlynn, S. and Matise, M. P. (2013). Floor plate-derived sonic hedgehog regulates glial and ependymal cell fates in the developing spinal cord. *Development* **140**, 1594-1604.

Zha, X. and Xu, X. (2015). Dissecting the hypothalamic pathways that underlie innate behaviors. *Neurosci. Bull.* **31**, 629-648.

Zhao, L., Kim, K. W., Ikeda, Y., Anderson, K. K., Beck, L., Chase, S., Tobet, S. A. and Parker, K. L. (2008). Central nervous system-specific knockout of steroidogenic factor 1 results in increased anxiety-like behavior. *Mol. Endocrinol.* **22**, 1403-1415.

Zhao, L., Zevallos, S. E., Rizzoti, K., Jeong, Y., Lovell-Badge, R. and Epstein, D. J. (2012). Disruption of SoxB1-dependent Sonic hedgehog expression in the hypothalamus causes Septo-optic Dysplasia. *Dev. Cell* **22**, 585-596.

Zhu, X., Gleiberman, A. S. and Rosenfeld, M. G. (2007). Molecular physiology of pituitary development: signaling and transcriptional networks. *Physiol. Rev.* **87**, 933-963.

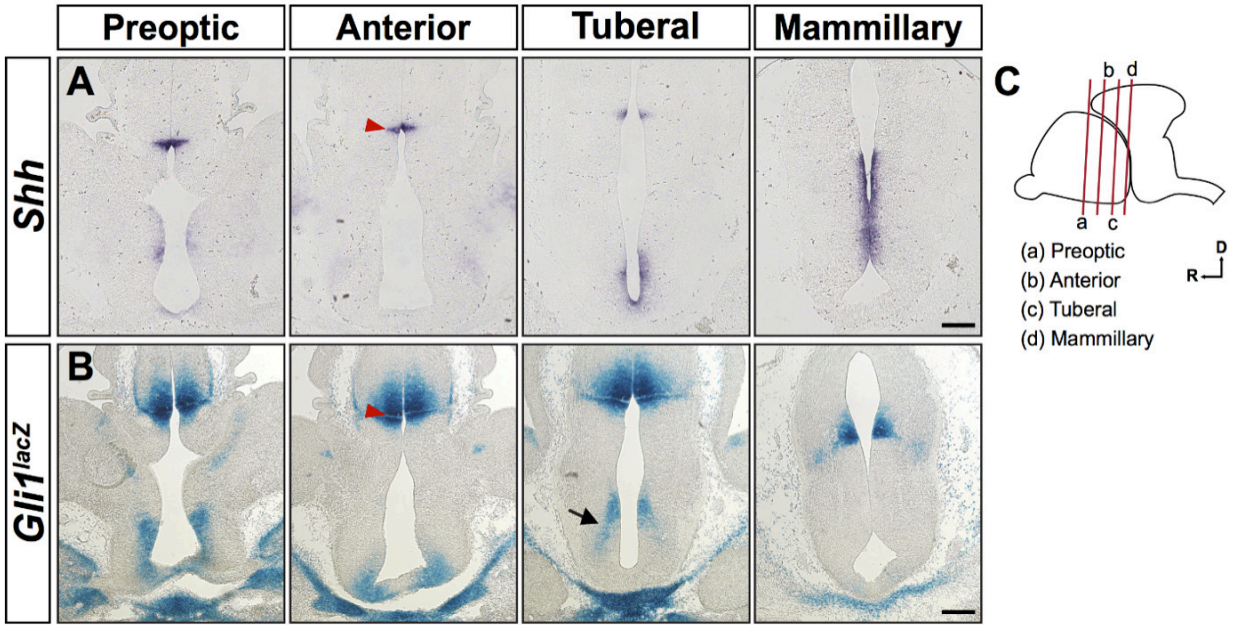

Figure S1. Persistence of *Shh* signaling during peak periods of hypothalamic neurogenesis. Coronal sections through the hypothalamus of (A) wild type and (B) *Gli1*$^{lacZ/+}$ embryos at E12.5. (A) RNA *in situ* hybridization detects *Shh* expression along the rostrocaudal axis of the hypothalamus. Weak *Shh* expression is detected in the ventral midline at preoptic and anterior hypothalamic regions. *Shh* expression is maintained in hypothalamic progenitors adjacent to the ventral midline in tuberal and mammillary regions. Shh is also observed in the zona limitans intrathalamica (red arrowhead) in the caudal diencephalon. (B) X-gal staining of *Gli1*^{lacZ} embryos along the rostrocaudal axis of the hypothalamus. X-gal staining is detected adjacent to Shh expressing domains throughout the hypothalamus. At the level of the tuberal hypothalamus, X-gal staining marks progenitors of the DMH and a population of cells that stream ventrally towards the VMH (arrows). Scale bars: 200 μm.

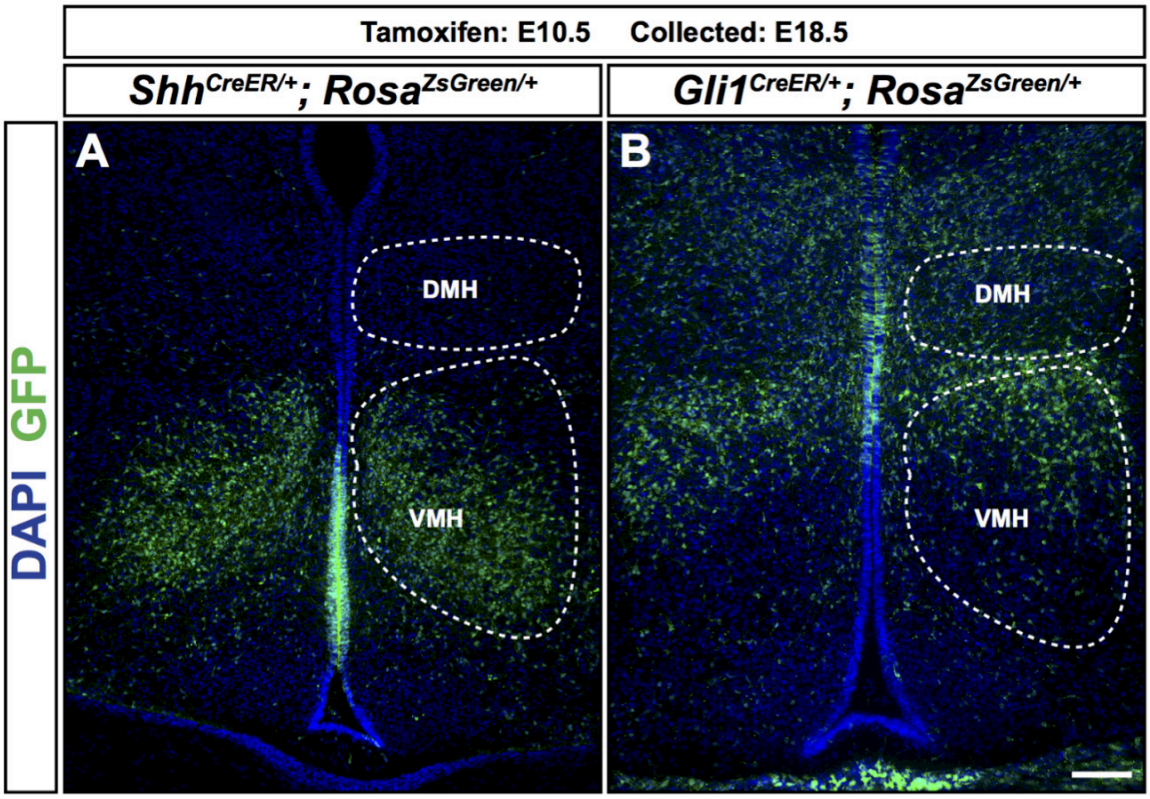

Figure S2. Shh and Gli1 lineages occupy distinct regions of the VMH. Coronal sections through the tuberal hypothalamus of (A) *Shh*$^{CreER/+}$; *Rosa*$^{ZsGreen/+}$ and (B) *Gli1*$^{CreER/+}$; *Rosa*$^{ZsGreen/+}$ embryos at E18.5 that received tamoxifen at E10.5. GFP (ZsGreen) fluorescence is shown on sections counterstained with DAPI. (A) Cells that expressed *Shh* at E10.5 contribute to the ventral and central regions of the VMH at E18.5. (B) Cells that expressed *Gli1* at E10.5 contribute to the DMH and dorsal region of the VMH at E18.5. Scale bar: 100 μm. White dashed lines outline tuberal hypothalamic nuclei.

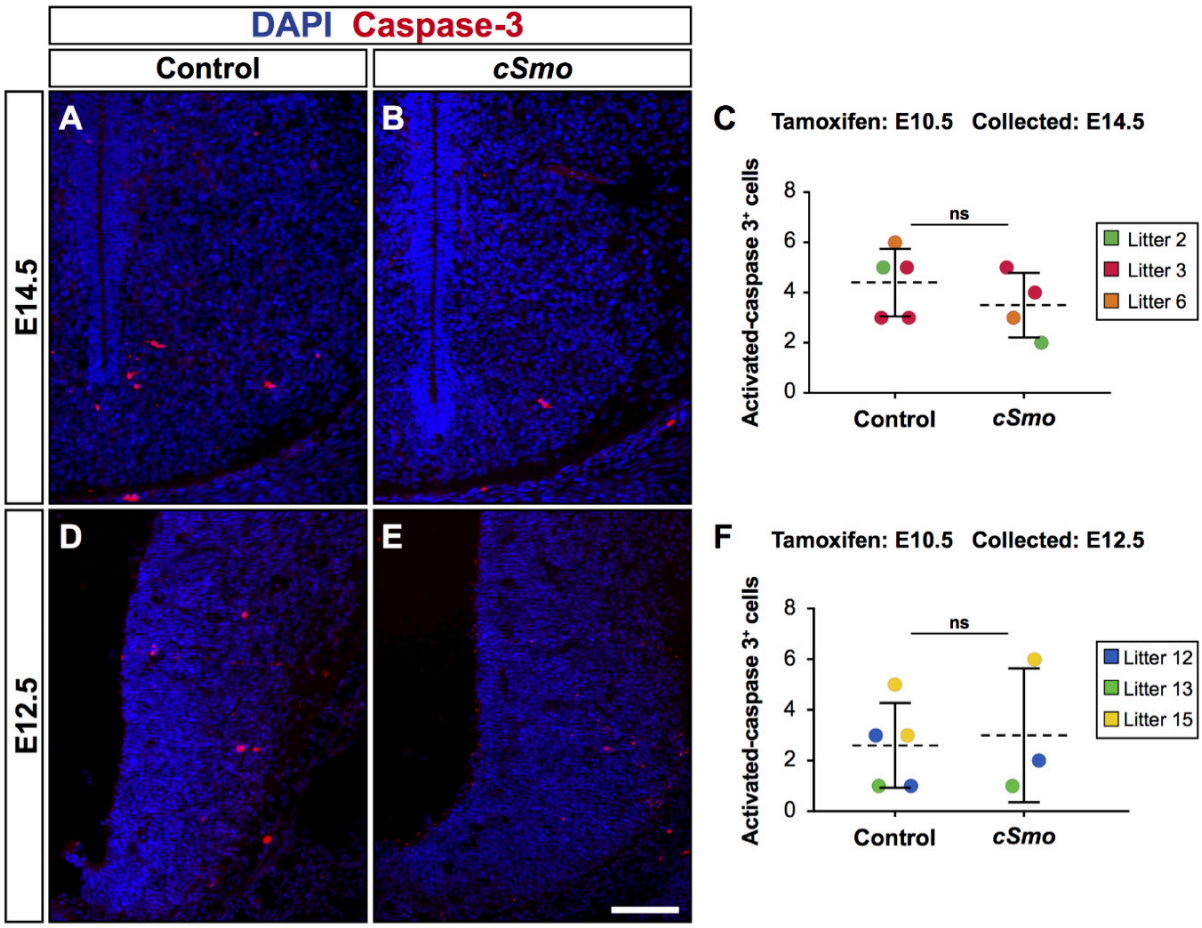

Figure S3. No difference in cell death between control and *cSmo* embryos. Coronal sections of control and *cSmo* embryos that received tamoxifen at E10.5 immunostained for activated caspase-3 and counterstained with DAPI. (A-C) No difference in apoptosis between control and *cSmo* embryos is observed at E14.5 (control n=5, 4.4 ± 1.3; *cSmo* n=4, 3.5 ± 1.3; p>0.05). (D-F) No difference in apoptosis between control and *cSmo* embryos is observed at E12.5 (control n=5, 2.6 ± 1.7; *cSmo* n=3, 3.0 ± 2.6; p>0.05). Each data point represents the number of cells expressing a given marker on a single section at equivalent levels of the tuberal hypothalamus from a single embryo color-coded by litter (n=number of embryos analyzed). Scale bars:100 µm. Statistical analysis was performed using a two-tailed unpaired *t*-test

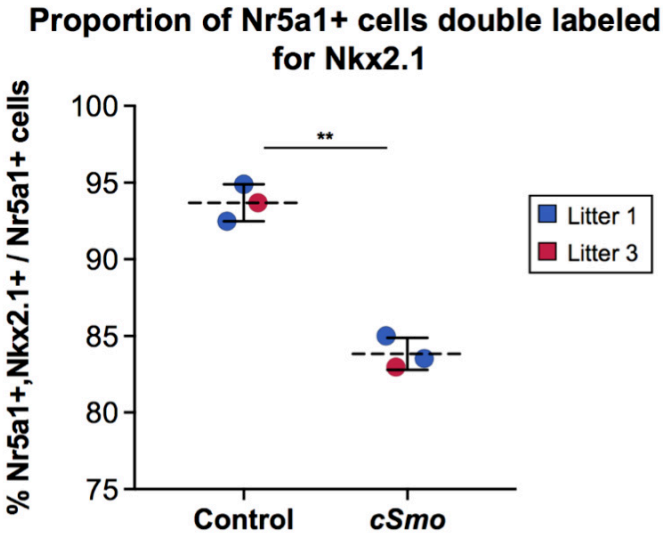

Figure S4. Fewer Nr5a1 expressing neurons co-label with Nkx2.1 in *cSmo* embryos. Quantification of Nr5a1 positive cells on a hemi-section double labeled for Nkx2.1 displayed as the proportion of Nr5a1, Nkx2.1 double positive cells over the total number of Nr5a1 positive cells (control n=3, 93.7% ± 0.7; *cSmo* n=3, 83.8% ± 0.6; **p=0.0004). Horizontal dotted line represents the mean and error bars indicate S.D. Statistical analysis was performed using a two-tailed unpaired *t*-test on arcsin-transformed data.

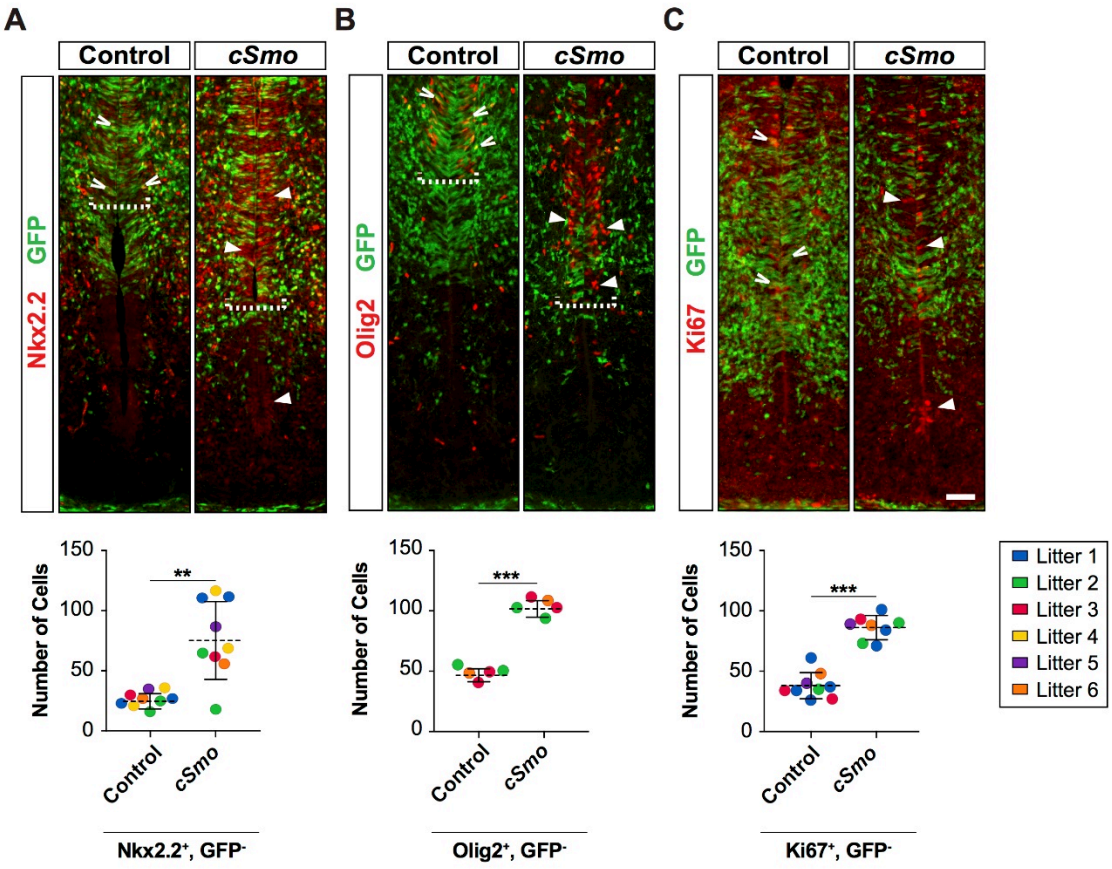

Figure S5. *cSmo* embryos show ectopic activation of Shh responsive genes in non-recombined (wild type) cells. Coronal sections through the tuberal hypothalamus of control and *cSmo* embryos at E14.5 (tamoxifen administered at E10.5). Shh responsive progenitors in control embryos frequently co-label with GFP and (A) Nkx2.2, (B) Olig2, or (C) Ki67 (open arrowhead). Most progenitors in *cSmo* embryos showing ectopic expression of Nkx2.2, Olig2, or Ki67 do not co-label with GFP (closed arrowheads), suggesting that they derive from non-recombined (wild type) cells. The ventral boundary of Nkx2.2 and Olig2 expression (white dotted bracket) is shifted ventrally in *cSmo* embryos. The same images are shown in Figure 6 without the GFP overlay. Scale bar: 50 μm.